

General framework for genuine multipartite entanglement detection

Xin-Yu Xu ^{1,2}, Qing Zhou ^{1,2}, Shuai Zhao ^{1,2}, Shu-Ming Hu ^{1,2}, Li Li ^{1,2,3,*}, Nai-Le Liu,^{1,2,3,†} and Kai Chen ^{1,2,3,‡}

¹*Hefei National Research Center for Physical Sciences at the Microscale and School of Physical Sciences, University of Science and Technology of China, Hefei 230026, China*

²*CAS Center for Excellence in Quantum Information and Quantum Physics, University of Science and Technology of China, Hefei 230026, China*

³*Hefei National Laboratory, University of Science and Technology of China, Hefei 230088, China*



(Received 10 December 2021; accepted 25 April 2023; published 12 May 2023)

The design of detection strategies for multipartite entanglement stands as a central importance on our understanding of fundamental quantum mechanics and has had a substantial impact on quantum information applications. However, accurate and robust detection approaches are severely hindered, particularly when the number of nodes grows rapidly like in a quantum network. Here we present a general and operational framework that generates alternative entanglement witness for an arbitrary targeted state. The framework enjoys a systematic and high-efficient character and allows to substantiate genuine multipartite entanglement for a variety of states that arise naturally in practical situations and to dramatically outperform currently standard methods. With excellent noise tolerance, our framework should be broadly applicable to witness genuine multipartite entanglement in various practically scenarios and to facilitate the best use of entangled resources in the emerging area of quantum network.

DOI: [10.1103/PhysRevA.107.052405](https://doi.org/10.1103/PhysRevA.107.052405)

I. INTRODUCTION

As a unique property in quantum theory, entanglement [1] is recognized as a kind of quantum resource [2] and plays a central role in numerous quantum computing and quantum communication tasks [3–7]. The ability to generate an increasing number of entangled particles is an essential benchmark for quantum information processing. In past decades, considerable efforts were made to prepare larger and more complex entangled states in various platforms [8–14], which in experimental systems are currently evolving from several qubits to noisy intermediate scale quantum system (NISQ) [15].

The developments of quantum technologies raise immediately important questions regarding the characterization of quantum entanglement of underlying systems. In bipartite systems, various theoretical works have contributed, such as separability criteria [16–19] and entanglement measures [20–22], which provide standard tools for characterizing bipartite entanglement. For some reviews, please refer to Refs. [1,23,24]. When it comes to multipartite systems, the problem is much more complicated. The entanglement structure becomes much richer for multipartite systems [25,26] since the number of possible divisions grows exponentially with the system size [1]. This leads to many types of multipartite entanglement, ranging from nonfully separable to genuine multipartite entanglement (GME). In the following, we focus

on the detection of genuine multipartite entanglement, which is an essential task for multipartite quantum communication and quantum computing tasks. For the detection of GME, many standard tools in the bipartite case, such as separability criteria, become infeasible since they only detect entanglement between two partitions. Meanwhile, a tomographic reconstruction of the quantum state required in these methods becomes time consuming and computationally difficult in the multipartite case.

For genuine multipartite entanglement detection, entanglement witness (EW) [27–31] provides an elegant solution both theoretically and experimentally without the need of having full tomographic knowledge about the state. Moreover, it is also known that the witness operator can be used to estimate entanglement measures [32]. On account of the simplicity and efficiency of entanglement witness, it has been widely used for experimental certification of GME in many platforms, such as trapped ions [33,34], photonic qubits [35–38], and superconducting qubits [39]. Most available GME witnesses are tailored towards some specific states, for instance, the Greenberger-Horne-Zeilinger (GHZ) states [40], W states [41], graph states [42,43], and so on. Despite a few general methods for the construction of GME witness being proposed [44–47], their performance is very limited, especially as the size of the system grows. One major drawback is the limited scope of noise resistance. For example, the fidelity-based method [44] is a canonical witness construction and widely used nowadays. Its noise tolerance decreases dramatically as the system size increases. In realistic NISQ systems, however, the noise always inevitably grows with the system size. In fact, it has been shown that the fidelity witnesses fail to detect a large amount of mixed entangled states [48]. To find more

*eidos@ustc.edu.cn

†nlliu@ustc.edu.cn

‡kaichen@ustc.edu.cn

robust GME witnesses, numerical methods were introduced [45], which, however, suffered from expensive computational costs as the system size grows. Hence, although it is known that for any entangled state there exists some EW to detect it [27], but how to construct a desirable EW to recognize a GME state is still a formidable challenge.

In this work, we propose a general framework to design robust GME witnesses by analytical and systematic construction. We start by introducing an operational method for lifting any set of bipartite EWs to construct GME witnesses. This establishes the link between the standard tools developed in the bipartite case and the GME witness construction. We then provide a well-designed class of optimal bipartite EWs that allows to design robust GME witnesses for arbitrary pure GME states. The performance of this framework on many typical classes of GME states is further evaluated in terms of white-noise tolerance. It can be shown that the framework outperforms the most widely used fidelity-based method with certainty and outperforms much better than the best-known EWs in many cases. Finally, benefiting from the high robustness of the resulting witnesses, we also demonstrate further applications of the framework, such as to provide a tighter lower bound on the genuine multipartite entanglement measures and detecting unfaithful GME states [48].

II. CONSTRUCTION OF ROBUST GME WITNESS

A. Preliminaries

To start with, we first give the precise definition of biseparable, genuine multipartite entanglement, and entanglement witness. A pure state is called *biseparable* if it can be written as a tensor product of two state vectors, i.e., $|\psi_A\rangle \otimes |\psi_{\bar{A}}\rangle$. Then a mixed state is called biseparable if it can be decomposed into a mixture of pure biseparable states, formally,

$$\rho_{bs} = \sum_{A|\bar{A},i} p_{A|\bar{A},i} |\psi_A^i\rangle\langle\psi_A^i| \otimes |\psi_{\bar{A}}^i\rangle\langle\psi_{\bar{A}}^i|, \quad (1)$$

where the summation can be performed over different bipartitions $A|\bar{A}$ of the entire system. A state that is not biseparable is referred to as genuine multipartite entangled. To detect the GME states, the most widely used method is to find an observable \mathcal{W}_{GME} that is nonnegative for all biseparable states and has a negative expectation value on at least one GME state. Then, for some multipartite quantum state ρ , the fact that $\text{Tr}(\mathcal{W}_{\text{GME}}\rho) < 0$ will reveal the existence of genuine multipartite entanglement and the \mathcal{W}_{GME} is called a *GME witness*. Moreover, given two EWs \mathcal{W}_1 and \mathcal{W}_2 , if there exists $\lambda > 0$ such that $\mathcal{W}_1 - \lambda\mathcal{W}_2$ is positive-semi-definite, i.e., $\mathcal{W}_1 \geq \lambda\mathcal{W}_2$, we say that \mathcal{W}_2 is *finer* than \mathcal{W}_1 [29]. The finer witness operator \mathcal{W}_2 detects more entangled states than \mathcal{W}_1 . An EW is *optimal* if no finer EW exists.

B. Design GME witness from a complete set of bipartite EWs

Due to its nonnegativity over all biseparable states, a GME witness \mathcal{W}_{GME} also serves as bipartite EW with respect to each possible bipartition of the entire system. In other words, there exists a complete set of bipartite EWs $\{\mathcal{W}_{A|\bar{A}}\}$ satisfying $\mathcal{W}_{\text{GME}} \geq \mathcal{W}_{A|\bar{A}}$ for each bipartition $A|\bar{A}$. This fact, from the opposite point of view, indicates that the GME witness \mathcal{W}_{GME}

is designed based on the set $\{\mathcal{W}_{A|\bar{A}}\}$ according to the constraint $\mathcal{W}_{\text{GME}} \geq \mathcal{W}_{A|\bar{A}}$. This naturally provides a general framework for constructing GME witnesses from a complete set of bipartite EWs. Remarkably, the set $\{\mathcal{W}_{A|\bar{A}}\}$ itself cannot be directly used to detect GME states as there exist biseparable states that are entangled with respect to every possible bipartition [23]. While there are two crucial issues with such a framework. The first one is how to find the operator satisfying $\mathcal{W}_{\text{GME}} \geq \mathcal{W}_{A|\bar{A}}$ and the second one is to decide which set of bipartite EWs should be used. The optimal solution to these two problems is hard, in general, and there have been only a few previous related studies on these issues [46,49,50]. In Ref. [46], an alternative solution was proposed to establish a connection between positive maps and multipartite EWs, where EWs detecting the multipartite bound entangled state were obtained. While in the following, we present an alternative solution that is capable of constructing robust GME witnesses.

C. Operational framework for GME witness construction

Any mixed GME state contains at least one pure GME state as a component, while the remaining components can be treated as noises. To detect mixed GME states with linear EW, it is natural to employ a witness operator for the pure GME component that is sufficiently robust to noise from the other components. In fact, the set of all optimal GME witnesses for all pure GME states will be sufficient to detect all GME states. However, finding all optimal GME witnesses is naturally a formidable task. Therefore, to advance a solution to this problem, we propose an operational framework to construct a class of robust GME witnesses for all pure GME states.

To address the problem of lifting any given set of bipartite EWs to multipartite, we can accomplish it in two steps. (1) For the first step, each bipartite EW $\mathcal{W}_{A|\bar{A}}$ is decomposed into some projectors. Note that the entanglement witness is designed for some pure entangled state $|\psi\rangle$. Hence we extract a term $-|\psi\rangle\langle\psi|$ before the decomposition. That is, the bipartite EWs are rewritten as $\mathcal{W}_{A|\bar{A}} = \mathcal{O}_{A|\bar{A}} - |\psi\rangle\langle\psi|$ and a spectral decomposition of $\mathcal{O}_{A|\bar{A}} = \mathcal{W}_{A|\bar{A}} + |\psi\rangle\langle\psi|$ is performed

$$\mathcal{O}_{A|\bar{A}} = \sum_{|\bar{v}_{i,A|\bar{A}}\rangle \in \mathcal{S}_{A|\bar{A}}} c_{i,A|\bar{A}} |\bar{v}_{i,A|\bar{A}}\rangle\langle\bar{v}_{i,A|\bar{A}}|, \quad (2)$$

with $\mathcal{S}_{A|\bar{A}}$ being the set of eigenvectors and $c_{i,A|\bar{A}}$ being the corresponding eigenvalues. All these eigenvectors are collected into a set $\mathcal{S} = \cup_{A|\bar{A}} \mathcal{S}_{A|\bar{A}}$. (2) For the second step, the obtained set \mathcal{S} is divided into m subsets $\{\mathcal{S}_k\}_{k=1}^m$ such that the vectors from different subsets are orthogonal with each other. Denote \tilde{I}_k as the identity operator on the subspace V_k spanned by the state vectors from subset \mathcal{S}_k and $c_k = \max_{|\bar{v}_{i,A|\bar{A}}\rangle \in \mathcal{S}_k} c_{i,A|\bar{A}}$ as the maximal coefficient attached to the state vectors in \mathcal{S}_k . With the above preparation and notation, we proceed to the following theorem.

Theorem 1. Given any pure GME state $|\psi\rangle$ and a set of bipartite EWs $\{\mathcal{W}_{A|\bar{A}}\}$ detecting $|\psi\rangle$ for all possible $A|\bar{A}$, the following operator $\hat{\mathcal{W}}$

$$\hat{\mathcal{W}} = \sum_{k=1}^m c_k \tilde{I}_k - |\psi\rangle\langle\psi|, \quad (3)$$

is nonnegative over all biseparable states, where the c_k and \tilde{I}_k are defined above.

Proof. To prove the statement, it suffices to observe

$$\begin{aligned} \hat{W} - \mathcal{W}_{A|\bar{A}} &= \sum_{k=1}^m c_k \tilde{I}_k - \mathcal{O}_{A|\bar{A}} \\ &= \sum_{k=1}^m \left(c_k \tilde{I}_k - \sum_{|v_{i,A|\bar{A}}\rangle \in \mathcal{S}_k \cap \mathcal{S}_{A|\bar{A}}} c_{i,A|\bar{A}} |\bar{v}_{i,A|\bar{A}}\rangle \langle \bar{v}_{i,A|\bar{A}}| \right) \\ &\geq \sum_{k=1}^m c_k \left(\tilde{I}_k - \sum_{|v_{i,A|\bar{A}}\rangle \in \mathcal{S}_k \cap \mathcal{S}_{A|\bar{A}}} |\bar{v}_{i,A|\bar{A}}\rangle \langle \bar{v}_{i,A|\bar{A}}| \right) \\ &\geq 0, \end{aligned} \tag{4}$$

where the inequalities can be derived directly from the definitions of c_k and \tilde{I}_k . ■

The above construction can be interpreted geometrically. That is, noise from different subspaces has different degrees of influence on the entanglement properties of the target state. The influence is characterized by the coefficients c_k and a small c_k indicates that noise from this subspace hardly affects the entanglement property of the target state. Therefore, Theorem 1 can be seen as a robust GME witness construction with the help of some prior knowledge of the target state, which comes from the set of bipartite EWs $\{\mathcal{W}_{A|\bar{A}}\}$.

Remarkably, Theorem 1 itself cannot be used as an operational framework for GME witness construction since the resulting operators can be positive-semi-definite and fail to detect any GME state. In fact, we can hardly expect a non-trivial result when the set of bipartite EWs $\mathcal{W}_{A|\bar{A}}$ are chosen randomly. Fortunately, standard tools exist for constructing bipartite EWs based on positive maps. In the following, to obtain an operational and general framework for GME witness construction, we provide a promising choice on the set of bipartite EWs, which is designed for the target states based on partial transposition.

Under any given bipartition $A|\bar{A}$, the target state $|\psi\rangle$ can be written in a Schmidt decomposition form $|\psi\rangle = \sum_{i=0}^{r_A-1} \sqrt{\lambda_{i,A|\bar{A}}} |i_A i_{\bar{A}}\rangle$, with r_A being the corresponding Schmidt rank. Note that here the local dimension of the Hilbert space need not be fixed. Then we introduce a class of bipartite EWs $\mathcal{W}_{o,A|\bar{A}}$ to use them in the construction of GME witness

$$\mathcal{W}_{o,A|\bar{A}} = \sum_{i,j=0}^{r_A-1} \sqrt{\lambda_{i,A|\bar{A}} \lambda_{j,A|\bar{A}}} |i_A j_{\bar{A}}\rangle \langle i_A j_{\bar{A}}| - |\psi\rangle \langle \psi|. \tag{5}$$

The choice of $\mathcal{W}_{o,A|\bar{A}}$ is mainly based on two considerations. First, $\mathcal{W}_{o,A|\bar{A}} + |\psi\rangle \langle \psi|$ naturally takes the decomposition form in the Eq. (2). Second, the above $\mathcal{W}_{o,A|\bar{A}}$ are a class of optimal bipartite EWs. For a detailed illustration and discussion on the $\mathcal{W}_{o,A|\bar{A}}$, please refer to Appendix A.

These bipartite EWs, together with Theorem 1, promise a general framework to construct GME witnesses with certainty. The explicit procedure is as follows.

(1) First, find the set \mathcal{S} . For each bipartition $M|\bar{M}$, calculate the Schmidt decomposition of $|\psi\rangle$ with respect to $M|\bar{M}$,

$$|\psi\rangle = \sum_{i=0}^{r_{M|\bar{M}}-1} \lambda_{i,M|\bar{M}} |\varphi_{i,M}\rangle |\varphi_{i,\bar{M}}\rangle, \tag{6}$$

with $r_{M|\bar{M}}$ being the Schmidt rank under this bipartition. A total of $r_{M|\bar{M}}^2$ vectors will be added to the set \mathcal{S} , and each of them given a corresponding coefficient. This is denoted by

$$\{(\sqrt{\lambda_{i,M|\bar{M}} \lambda_{j,M|\bar{M}}}, |\varphi_{i,M}\rangle |\varphi_{j,\bar{M}}\rangle)\}_{i,j=0}^{r_{M|\bar{M}}-1}. \tag{7}$$

After going through all possible bipartitions, we will end up with a set of vectors \mathcal{S} as well as their corresponding coefficients.

(2) Second, find the finest division of \mathcal{S} such that vectors from different subsets are orthogonal with each other. This can be achieved with the following steps.

- (i) Put the first element of \mathcal{S} into an empty subset \mathcal{S}_1 .
- (ii) For every other vector in $\mathcal{S} - \mathcal{S}_1$, if it is not orthogonal with all vectors in the set \mathcal{S}_1 , it is added into \mathcal{S}_1 . Repeat this step until no new vector can be added to \mathcal{S}_1 .
- (iii) For the rest of the vectors in $\mathcal{S} - \mathcal{S}_1$, repeat the above two steps to obtain $\mathcal{S} - \mathcal{S}_1 - \mathcal{S}_2$, $\mathcal{S} - \mathcal{S}_1 - \mathcal{S}_2 - \mathcal{S}_3$, ..., until all the elements of \mathcal{S} are classified.
- (iv) A division $\mathcal{S} = \sum_{k=1}^m \mathcal{S}_k$ is obtained.

(3) Third, calculate the subspace spanned by the vectors in subset \mathcal{S}_k . By performing Schmidt orthogonalization of the vectors in \mathcal{S}_k , we can derive the subspace spanned by these vectors and obtain the identity operator \tilde{I}_k on this subspace.

(4) Finally, for each subset \mathcal{S}_k , find the maximal coefficients c_k attached to the vectors in it and construct a GME witness using Theorem 1.

There are two remarks to note about this method. First, the resulting witness from the above procedure is always finer than the commonly used GME fidelity witness $\mathcal{W}_F = \lambda I - |\psi\rangle \langle \psi|$ for $|\psi\rangle$, with $\lambda = \max_{A|\bar{A}} \lambda_{0,A|\bar{A}}$ (here it is assumed that the Schmidt coefficients $\lambda_{i,A|\bar{A}}$ are in decreasing order). To illustrate this, note that if the bipartite EWs are chosen as the bipartite fidelity witness $\mathcal{W}_{F,A|\bar{A}} = \lambda_{0,A|\bar{A}} I - |\psi\rangle \langle \psi|$, by applying Theorem 1, the obtained operator is nothing but the \mathcal{W}_F . Whereas by checking $\mathcal{W}_{F,A|\bar{A}} - \mathcal{W}_{o,A|\bar{A}} \geq 0$, it is straightforward to verify that the above $\mathcal{W}_{o,A|\bar{A}}$ is finer than the bipartite fidelity witness $\mathcal{W}_{F,A|\bar{A}}$. Therefore, when Theorem 1 is applied to the set of $\mathcal{W}_{o,A|\bar{A}}$, the resulting GME witness strictly outperforms the corresponding fidelity witness \mathcal{W}_F . Second, we start from a complete set of bipartite EWs in the above construction, leading to EWs that detect genuine multipartite entanglement. While if one starts from a smaller set of bipartite EWs, the method allows also for flexible applications in verifying other kinds of multipartite entanglement, e.g., characterizing the entanglement depth.

III. EXAMPLES

To help obtain a better understanding as well as quantitatively investigating the robustness of the framework, we proceed to some explicit examples, where the white-noise tolerance is employed as a figure of merit to evaluate its performance in practice. The white-noise tolerance of some

witness operator \mathcal{W} for $|\psi\rangle$ is the critical value of p such that the mixed state $pI/d + (1-p)|\psi\rangle\langle\psi|$ is not detected by \mathcal{W} .

A. W state

To investigate the asymptotic behavior of this framework with an increasing system size, we start with the n -qubit W state $|W_n\rangle = (|00\cdots 01\rangle + |00\cdots 10\rangle + \cdots + |10\cdots 00\rangle)/\sqrt{n}$, which is widely used in quantum information processing tasks. For the W state, we find the GME witness (see Appendix B 1 for a proof)

$$\mathcal{W}_{|W_n\rangle} = \frac{n-1}{n}\mathcal{P}_1^n + \frac{\sqrt{\lfloor n/2\rfloor(n-\lfloor n/2\rfloor)}}{n}(\mathcal{P}_0^n + \mathcal{P}_2^n) - |W_n\rangle\langle W_n|, \quad (8)$$

with $\mathcal{P}_i^n = \sum_m \pi_m(|0\rangle^{\otimes n-i}|1\rangle^{\otimes i})\pi_m(\langle 0|^{\otimes n-i}\langle 1|^{\otimes i})$, where the summation m is over all possible permutations of $|0\rangle^{\otimes n-i}|1\rangle^{\otimes i}$. The $\mathcal{W}_{|W_n\rangle}$ recovers a class of EWs presented in Ref. [51], which are the most powerful ones for the W state presently. Its white-noise tolerance also tends to 1 for an increasing number of qubits. While for the fidelity witness, its white-noise tolerance is $1/[n(1-1/2^n)]$, tending to $1/n$ for large n .

B. Graph state

Graph states are a class of genuine multipartite entangled states that are of great importance for measurement-based quantum computation [52], quantum error correction [53], and so on. In Refs. [45,54], the authors developed powerful entanglement witnesses for graph states. Our framework suggests that there is still much room for improvement in the robustness of these existing results.

More specifically, we focus on a typical class of graph state: the n -qubit ($n \geq 4$) linear cluster states $|Cl_n\rangle$ in this example. The $|Cl_n\rangle$ can be expressed by a set of stabilizers $\{g_i\}_{i=1}^n$, with $g_i = Z_{i-1}X_iZ_{i+1}$ ($2 \leq i \leq n-1$), $g_1 = X_1Z_2$, and $g_n = Z_{n-1}X_n$, respectively, where the X and Z are Pauli operators. All the common eigenstates of these stabilizers introduce a complete basis, i.e., the graph-state basis. This basis can be denoted by $|\vec{a}\rangle_{Cl_n}$, with $\vec{a} = a_1a_2\cdots a_n \in \{0, 1\}^n$, such that $g_i|\vec{a}\rangle_{Cl_n} = (-1)^{a_i}|\vec{a}\rangle_{Cl_n}$ for $i = 1, \dots, n$. Specifically, the $|Cl_n\rangle$ corresponds to $|00\cdots 0\rangle_{Cl_n}$. When applied to the linear cluster state, our framework results in a GME witness which is diagonal under the graph state basis (for the explicit construction process, we refer to Appendix B 2)

$$\mathcal{W}_{Cl_n} = \sum_{k=1}^{\lfloor n/3 \rfloor} \sum_{\vec{a} \in V_k} \frac{1}{2^k - 1} |\vec{a}\rangle_{Cl_n} \langle \vec{a}| - |Cl_n\rangle \langle Cl_n|. \quad (9)$$

Here a vector \vec{a} belongs to V_k if there exist at most k for the number of “1”s in \vec{a} , such that their distance with each other are larger than 2 at the same time (for instance, 1101100 belongs to V_2 while 1001011 belongs to V_3). Its white-noise tolerance p_{Cl_n} of the \mathcal{W}_{Cl_n} is presented in Fig. 1. It is observed that the \mathcal{W}_{Cl_n} can outperform the best-known class of EWs provided in the Ref. [45] for $n > 5$. Meanwhile, the white-noise tolerance p_{Cl_n} exhibits a similar asymptotic behavior as in the first example, that is, tending to 1 for large n . We remark that while the resulting EWs are quite robust, they are not optimal. In fact, the optimality of the bipartite EWs employed

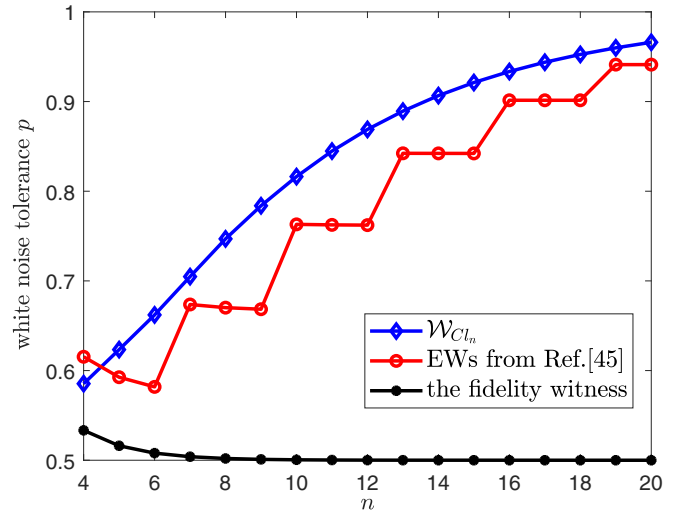


FIG. 1. In this figure we illustrate the performance of \mathcal{W}_{Cl_n} by showing its white noise tolerance for n -qubit cluster state up to 20 qubits. It is plotted with a blue line with diamonds. As a comparison, the red circle line is the best-known result introduced in Ref. [45]. Remarkably, the result in this paper outperforms this existing EW since the number of qubit is larger than 5. Both of their white-noise tolerance tends to 1. For the widely used fidelity witness of $|Cl_n\rangle$, its white-noise tolerance is given by the black line with filled circles tending to $1/2$ with an increasing qubit number.

in the construction is not sufficient to guarantee the optimality of the resulting GME witness. For some explicit target states, we may either analytically or numerically optimize the result. However, a systematic and operational improvement of this framework remains an open problem. A brief discussion on this issue is provided at the end of Appendix B 2.

C. Multipartite states admitting Schmidt decomposition

In the above examples, we benchmark our method with some well-studied states. Now we turn to other less-investigated states, where this method remains powerful. A typical class is the multipartite states admitting Schmidt decomposition. Without loss of generality, such a state takes the form $|\phi_s\rangle = \sum_{i=0}^{d-1} \sqrt{\lambda_i} |i\rangle^{\otimes n}$, where the λ_i are in decreasing order. This class of states includes high-dimensional GHZ states $|\text{GHZ}_n^d\rangle = \sum_{i=0}^{d-1} |i\rangle^{\otimes n} / \sqrt{d}$ as a typical case when all the Schmidt coefficients are equal. For the multipartite states admitting Schmidt decomposition, our method leads to a class of optimal EWs (see Appendix B 3 for a proof)

$$\mathcal{W}_{|\phi_s\rangle} = \sum_{\substack{i,j=0, \\ i < j}}^{d-1} \sum_{r=1}^{n-1} \sum_m \sqrt{\lambda_i \lambda_j} \pi_m(|i\rangle^{\otimes r} |j\rangle^{\otimes n-r}) \pi_m(\langle i|^{\otimes r} \langle j|^{\otimes n-r}) + \sum_{i=0}^{d-1} \lambda_i |i\rangle \langle i|^{\otimes n} - |\phi_s\rangle \langle \phi_s|, \quad (10)$$

where $\pi_m(|i\rangle^{\otimes r} |j\rangle^{\otimes n-r})$ is a permutation of $|i\rangle^{\otimes r} |j\rangle^{\otimes n-r}$ and the summation of m is over all possible permutations. The white-noise tolerance of $\mathcal{W}_{|\phi_s\rangle}$ is $p_{\mathcal{W}_{|\phi_s\rangle}} = (1 - \sum_{i=0}^{d-1} \lambda_i^2) / \{1 - \sum_{i=0}^{d-1} \lambda_i^2 + \frac{2^{n-1}-1}{d^n} [(\sum_{i=0}^{d-1} \sqrt{\lambda_i})^2 - 1]\}$.

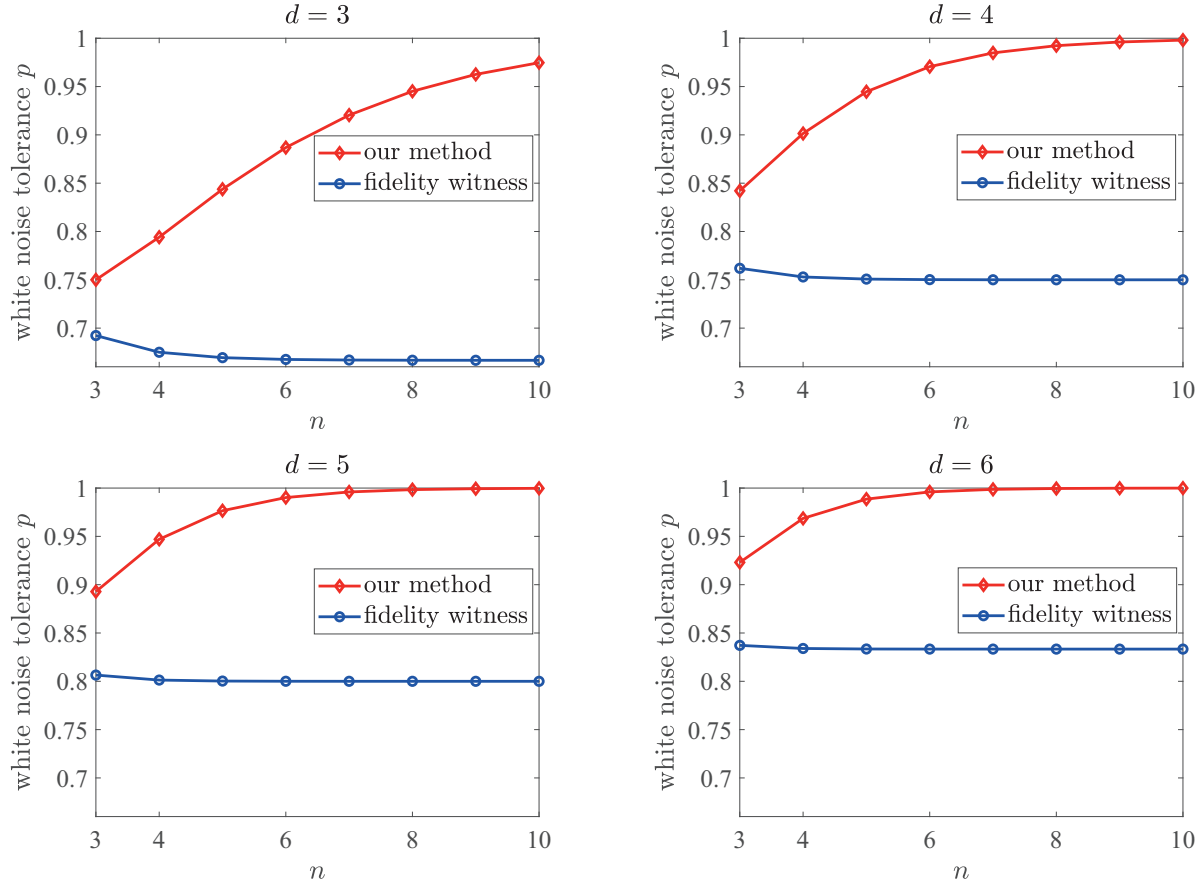


FIG. 2. In this figure, we show how the white-noise tolerance of different EWs varies with an increasing qudit number n , with $d = 3, 4, 5, 6$, respectively. The target states are d -dimensional GHZ states, which belong to the class of states in Example 1. In each subfigure, the white-noise tolerance of the GME witness in Eq. (10) is plotted by red line with diamonds, and in comparison the white-noise tolerance of the normal fidelity witness $\mathcal{W}_F^{|\psi_s\rangle} = I/d - |\text{GHZ}_n^d\rangle\langle\text{GHZ}_n^d|$ is plotted by blue circled line. As observed in this figure, for all local dimension $d \geq 3$, our results increase and converge to 1 with the increasing system size. While for the normal fidelity witness, its white-noise tolerance decreases when the number of qudits grows and eventually tends to $1 - 1/d$.

The $p_{\mathcal{W}^{|\psi_s\rangle}}$ tends to 1 for large n when $d > 2$. As a comparison, the best-known GME witness for this kind of state comes from the fidelity-based method, with $\mathcal{W}_F^{|\psi_s\rangle} = \lambda_0 I - |\phi_s\rangle\langle\phi_s|$. The white-noise tolerance of $\mathcal{W}_F^{|\psi_s\rangle}$ is $(1 - \lambda_0)/(1 - 1/d^n)$, which tends to $1 - \lambda_0 \leq 1 - 1/d$ with an increasing system size. For the special case of n -qudit GHZ states $|\text{GHZ}_n^d\rangle$, the performance of our construction and the fidelity-based method is compared in Fig. 2, where a significant improvement is demonstrated. Note that for n -qudit GHZ states $|\text{GHZ}_n^d\rangle$, the fidelity witness is already optimal, and hence we start from the local dimension $d = 3$ in Fig. 2.

D. Four-qubit singlet state

Multiqubit singlet states are another interesting family of multiqubit states. They are invariant under a simultaneous unitary rotation on all qubits ($U^{\otimes n}|\psi\rangle\langle\psi|(U^\dagger)^{\otimes n} = |\psi\rangle\langle\psi|$). In the four-qubit case, all four-qubit singlet states live in a two-dimensional subspace of the entire Hilbert space. Without loss of generality, it can be denoted as

$$|\varphi_4\rangle = a|\psi_{12}^-\rangle \otimes |\psi_{34}^-\rangle + e^{i\theta}b|\psi_{13}^-\rangle \otimes |\psi_{24}^-\rangle, \quad (11)$$

with the constraint $a^2 + b^2 + \cos(\theta)ab = 1$ and $|\psi_{12}^-\rangle$ being the two-qubit singlet state $(|01\rangle - |10\rangle)/\sqrt{2}$ on the first two qubits. Specifically, for the choice of $\theta = \pi/2$, we arrive at a class of four-qubit singlet states decided by a single parameter $|\varphi_4(a)\rangle = a|\psi_{12}^-\rangle \otimes |\psi_{34}^-\rangle + i\sqrt{1 - a^2}|\psi_{13}^-\rangle \otimes |\psi_{24}^-\rangle$ with $a \in [-1, 1]$. For this class of state $|\varphi_4(a)\rangle$, our framework results in the following GME witness:

$$\mathcal{W}_4(a) = \alpha\mathcal{P}_2^4 + \frac{1}{2}(\mathcal{P}_1^4 + \mathcal{P}_3^4) + \frac{1}{4}(\mathcal{P}_0^4 + \mathcal{P}_4^4) - |\varphi_4\rangle\langle\varphi_4|, \quad (12)$$

where $\alpha = \max\{[1 + 3(1 - a^2)]/4, (1 + 3a^2)/4\} \geq 5/8$. While the fidelity-based witness for such state is $\mathcal{W}'_4(a) = \alpha I - |\varphi_4\rangle\langle\varphi_4|$. In Appendix B 4, a further discussion of the entanglement detection for multiqubit singlet states is proposed based on our framework.

Consequently, we provided a general framework for detecting arbitrary target GME state in a noisy system by constructing robust GME witnesses. First, by benchmarking its performance on some well-studied states, it is observed that this framework results in robust GME witnesses that perform comparable to the current best witnesses for these states. For other less-investigated states, the most widely used method

to construct EW for them is the fidelity-based method. As shown in these examples, our framework can provide a significant improvement compared with the fidelity-based method. This also leads to the conjecture that a large amount of pure GME states become fairly robust to noise as the system size increases. Second, the advantage of our framework against the fidelity-based method comes with no experimental overheads. This benefits from the fact that the $\sum_k c_k \tilde{I}_k$ term in this construction is usually diagonal in some well-defined basis, such as the graph-state basis and the computational basis. Finally, it should be stressed that Theorem 1 can be applied not only to the class of bipartite EWs shown in Eq. (5), but also to other classes of bipartite EWs. This potentially results in some different GME witnesses. A further example is provided in Appendix A 3.

IV. APPLICATIONS OF THE RESULTING GME WITNESSES

A. Detection of unfaithfulness

The unfaithful entangled states are a large class of states that cannot be recognized with any fidelity witness and have attracted both theoretical and experimental interests [55–58]. Therefore, given that we already gained access to construct finer GME witnesses than the fidelity-based method, it is natural to investigate their ability on the detection of unfaithful GME states.

In general, deciding whether an entangled state is unfaithful is a nontrivial task since one has to prove that the state is not detected by all fidelity witnesses rather than a certain one. In the bipartite case, a necessary and sufficient criterion for a state ρ_{AB} to be unfaithful was proposed [55], while for the multipartite case, the characterization of unfaithfulness remains an open problem. To avoid this difficulty and verify that an EW indeed detects unfaithfulness, we limit our attention to a special class of states $\rho(p) = pI/d^n + (1-p)\rho_0$ to show that there is an upper bound on the white-noise tolerance of any fidelity witness for arbitrary state. Denote $\mathcal{W}_F = \alpha I - \rho'$ as an arbitrary fidelity witness, then we can derive its white-noise tolerance p_F for arbitrary $\rho(p)$ by solving $\text{Tr}[\mathcal{W}_F \rho(p)] = 0$, which leads to

$$p_F = \max \left\{ \frac{\text{Tr}(\rho_0 \rho') - \alpha}{\text{Tr}(\rho_0 \rho') - 1/d^n}, 0 \right\}. \quad (13)$$

Then it is straightforward to see that $p_F \leq (1 - 1/d)/(1 - 1/d^n)$ due to the fact that $\text{Tr}(\rho_0 \rho') \leq 1$ and $\alpha \geq 1/d$. Hence it can be concluded that an EW can be employed to detect some unfaithful entangled states as long as its white-noise tolerance for some state is higher than $(1 - 1/d)/(1 - 1/d^n)$. This is precisely the case for many GME witnesses constructed with our framework. For example, in an n -qubit case, this upper bound is $1/[2(1 - 1/2^n)]$ and decreases to $1/2$ as n grows. While our framework provides large amount of EWs with white-noise tolerance converging to 1, this allows for the certification of unfaithfulness of many states in n -qubit case.

B. Estimating entanglement measures

Moreover, a witness operator is useful not only for entanglement certification, but also for entanglement quantification.

To start with, we briefly review the method developed in Ref. [32] for optimally estimating some entanglement measure E given the expectation value of some witness operator \mathcal{W} . The task can be described as finding the lower bound

$$\varepsilon(w) = \inf_{\rho} \{E(\rho) | \text{Tr}(\rho \mathcal{W}) = w\}, \quad (14)$$

where the infimum is taken over all states compatible with the data $w = \text{Tr}(\rho \mathcal{W})$. Note that $\varepsilon(w)$ is a convex function and thus there exist bounds of the type

$$\varepsilon(w) \geq rw - c, \quad (15)$$

for an arbitrary r . By inserting $w = \text{Tr}(\rho \mathcal{W})$ and $E(\rho) \geq \varepsilon(w)$, it is observed that

$$c \geq r \text{Tr}(\rho \mathcal{W}) - E(\rho), \quad (16)$$

should be satisfied for any ρ . Hence given a ‘‘slope’’ r , the optimal constant c is

$$c = \hat{E}(r\mathcal{W}) := \sup_{\rho} \{r \text{Tr}(\rho \mathcal{W}) - E(\rho)\}. \quad (17)$$

Finally, an optimal lower bound is obtained after optimizing r :

$$\varepsilon(w) = \sup_r \{rw - \hat{E}(r\mathcal{W})\}. \quad (18)$$

Here we limit our discussions into the nontrivial case, where a negative expectation w of a witness operator is observed. In this case, the optimal ‘‘slope’’ r is always negative.

Now, suppose that the \mathcal{W}_2 is a finer EW than the \mathcal{W}_1 , satisfying $\mathcal{W}_2 \leq \mathcal{W}_1$. It is straightforward to see that

$$\hat{E}(r\mathcal{W}_1) \geq \hat{E}(r\mathcal{W}_2). \quad (19)$$

Therefore, when these two operators \mathcal{W}_1 and \mathcal{W}_2 have the same expectation value w_0 ,

$$\begin{aligned} \varepsilon_2(w_0) &= \sup_r \{rw_0 - \hat{E}(r\mathcal{W}_2)\} \\ &\geq \sup_r \{rw_0 - \hat{E}(r\mathcal{W}_1)\} \\ &= \varepsilon_1(w_0). \end{aligned} \quad (20)$$

For the same target state ρ , the expectations w_1 and w_2 of these two witness operators always satisfy $w_1 \geq w_2$, which leads to $\varepsilon_2(w_2) \geq \varepsilon_2(w_1) \geq \varepsilon_1(w_1)$. That is, a finer EW provides a tighter lower bound on the entanglement measure for the same state. Hence, our framework enables a better estimation of the entanglement measures of genuine multipartite entanglement than the fidelity-based method.

To quantitatively investigate the improvement from these new GME witness, we discuss the estimation on the geometry measure of genuine multipartite entanglement for noisy n -partite d -dimensional GHZ states $\rho_{n,d}(p) = pI/d^n + (1-p)|\text{GHZ}_n^d\rangle\langle\text{GHZ}_n^d|$, with $|\text{GHZ}_n^d\rangle = \sum_{i=0}^{d-1} |i\rangle^{\otimes n} / \sqrt{d}$. For the arbitrary multipartite pure state $|\psi\rangle$, its geometric measurement of GME is defined by $E_G(|\psi\rangle) = 1 - \max_{|\phi_{bs}\rangle} |\langle\phi_{bs}|\psi\rangle|^2$, with $|\phi_{bs}\rangle$ being an arbitrary pure biseparable state. The geometric measure of GME is extended to mixed states by the convex roof construction

$$E_G(\rho) = \inf_{p_i, |\psi_i\rangle} \sum_i p_i E_G(|\psi_i\rangle), \quad (21)$$

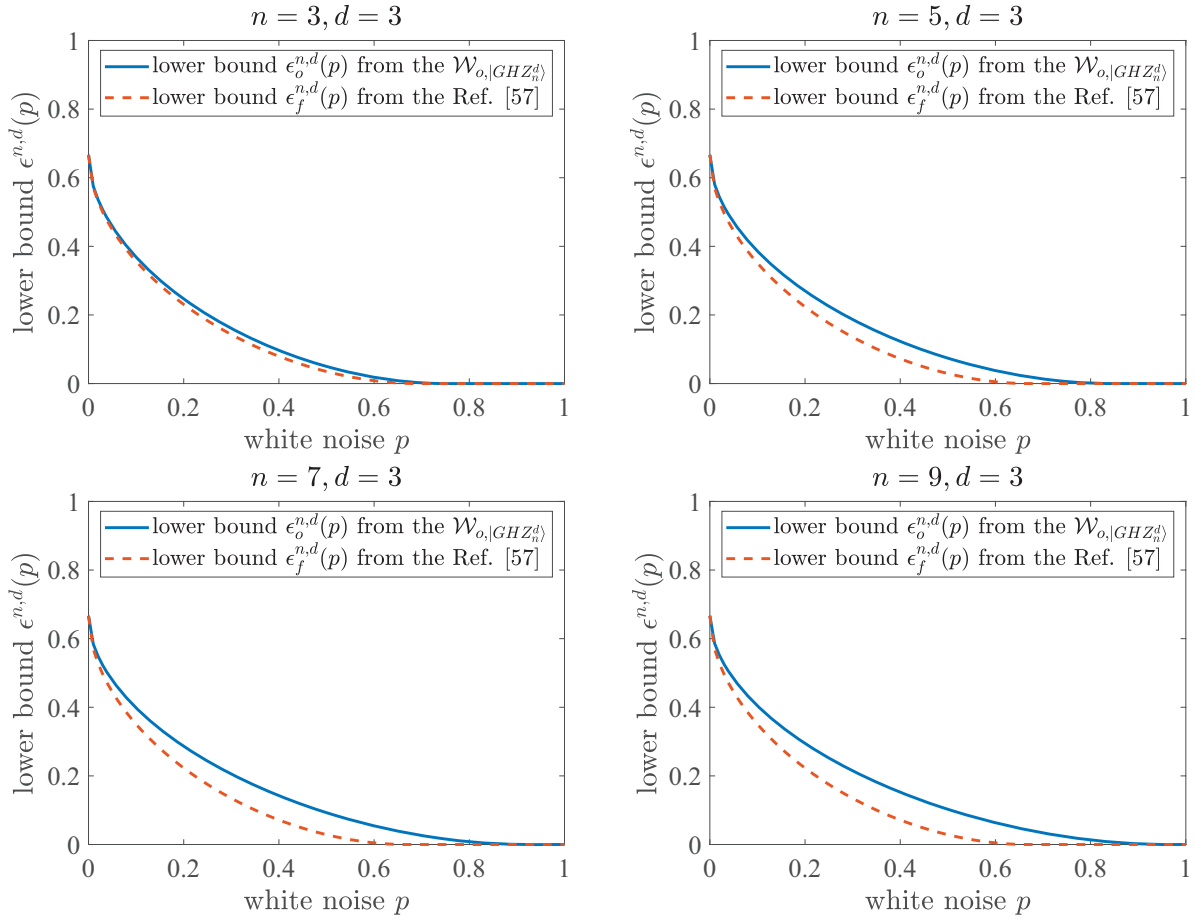


FIG. 3. In this figure, we choose $d = 3$ and $n = 3, 5, 7, 9$ as examples to compare the lower bound $\varepsilon_o^{n,d}(p)$ (solid blue line) and $\varepsilon_f^{n,d}(p)$ (dashed red line) of geometric measure of GME from different EWs. It is observed that the advantage of EWs in this work become more apparent with increasing system size. Note that, for higher local dimensions where $d \geq 4$, the lower bound $\varepsilon_o^{n,d}(p)$ and $\varepsilon_f^{n,d}(p)$ have similar behavior. While in the qubit case, the EW $\mathcal{W}_{\alpha,|\text{GHZ}_n^d\rangle}$ degenerates to the fidelity witness $I/2 - |\text{GHZ}_n\rangle\langle\text{GHZ}_n|$ for n -qubit GHZ state $|\text{GHZ}_n\rangle$, and $\varepsilon_o^{n,2}(p)$ is the same as $\varepsilon_f^{n,2}(p)$.

where the minimization runs over all possible decompositions $\rho = \sum_i p_i |\psi_i\rangle\langle\psi_i|$.

Based on the result in Ref. [59], we can derive a lower bound $\varepsilon_f^{n,d}(p)$ for $E_G[\rho_{n,d}(p)]$

$$E_G[\rho_{n,d}(p)] \geq \varepsilon_f^{n,d}(p) := 1 - \gamma(S), \quad (22)$$

where $\gamma(S) = [\sqrt{S} + \sqrt{(d-1)(d-S)}]^2/d$ with $S = \max\{1, d(1-p) + p/d^{n-1}\}$. This is just the lower bound related to the fidelity witness $\mathcal{W}_F = I/d - |\text{GHZ}_n^d\rangle\langle\text{GHZ}_n^d|$. Whereas it is proved in the previous section that finer EW is accessible with our method, that is,

$$\begin{aligned} \mathcal{W}_{\alpha,|\text{GHZ}_n^d\rangle} &= \sum_{\substack{i,j=0 \\ i < j}}^{d-1} \sum_{r=1}^{n-1} \sum_m \frac{1}{d} \pi_m(|i\rangle^{\otimes r} |j\rangle^{\otimes n-r}) \pi_m(\langle i|^{\otimes r} \langle j|^{\otimes n-r}) \\ &+ \sum_{i=0}^{d-1} \frac{1}{d} |i\rangle\langle i|^{\otimes n} - |\text{GHZ}_n^d\rangle\langle\text{GHZ}_n^d|. \end{aligned} \quad (23)$$

With the expectation value $w_{n,d}(p) = \text{Tr}[\rho_{n,d}(p)\mathcal{W}_{\alpha,|\text{GHZ}_n^d\rangle}]$ from this finer EW, a lower bound $\varepsilon_o^{n,d}(p)$ can be derived by

employing the technique developed in Ref. [32]

$$E_G[\rho_{n,d}(p)] \geq \varepsilon_o^{n,d}(p) := \sup_r \{r w_{n,d}(p) - \hat{E}_G(r\mathcal{W}_{\alpha,|\text{GHZ}_n^d\rangle})\}, \quad (24)$$

with r being a real number and

$$\begin{aligned} \hat{E}_G(r\mathcal{W}_{\alpha,|\text{GHZ}_n^d\rangle}) &= \sup_{|\psi\rangle} \sup_{|\phi_{bs}\rangle} \{ \langle\psi|(r\mathcal{W}_{\alpha,|\text{GHZ}_n^d\rangle} + |\phi_{bs}\rangle\langle\phi_{bs}|)|\psi\rangle - 1 \}, \end{aligned} \quad (25)$$

where the maximization runs over all pure state $|\psi\rangle$ and biseparable state $|\phi_{bs}\rangle$. Furthermore, in this special case, it can be verified that one has to choose $|\phi_{bs}\rangle$ as a state having the largest overlap with $|\text{GHZ}_n^d\rangle$, which results in

$$\hat{E}_G(r\mathcal{W}_{\alpha,|\text{GHZ}_n^d\rangle}) = \frac{1-r}{2} + \frac{1}{2} \sqrt{(1-r)^2 + 4r \frac{d-1}{d}} + \frac{r}{d} - 1. \quad (26)$$

By inserting this equation into Eq. (24), the lower bound $\varepsilon_o^{n,d}(p)$ can be solved directly.

In Fig. 3, we show the results for $d = 3$ and $n = 3, 5, 7, 9$ as examples, to illustrate the performance of our method

with an increasing system size. As the number of subsystems grows, the critical value of p tends to 1, when the lower bound $\varepsilon_o^{n,d}(p)$ vanishes. Meanwhile, the $\varepsilon_o^{n,d}(p)$ is always larger than the $\varepsilon_f^{n,d}(p)$ above, which vanishes at $p = 1 - 1/d$ for large n . That is, the new EWs $\mathcal{W}_{\alpha,|\text{GHZ}_n^d\rangle}$ are able to provide a better estimation on the geometric measure of GME for $\rho_{n,d}(p)$. It remains open whether $\varepsilon_o^{n,d}(p)$ equals $E_G[\rho_{n,d}(p)]$. However, it is still reasonable to expect that such new GME witnesses can provide faithful estimations on entanglement measures without the need for quantum tomography, as they are already robust enough.

V. CONCLUSION AND OUTLOOK

In summary, we developed a general framework for genuine multipartite entanglement detection around any given target state and demonstrated its operability and universality by applying it on typical GME states that arise in practice. In particular, this is achieved using a method to bring any complete set of bipartite EWs to a single GME witness. This method allows to make full use of some prior information about the target state to improve the noise resistance. In fact, the resulting GME witnesses turn out to be quite robust and whose white-noise tolerance converge to 1 in many cases. As a consequence, this framework holds great practical potential in real-life situations, particularly for detecting entanglement in noisy multipartite or high-dimensional systems. This will play a certain role in facilitating the solution of the very challenging problem of genuine multipartite entanglement detection.

In addition to genuine multipartite entanglement, we remark that our method is highly flexible and admits natural generalizations for detecting other types of entanglement. A relevant case is entanglement detection in quantum networks, which is currently under active investigation. In quantum networks, multipartite entanglement exhibits novel features due to the complex network topology [60–62] and better techniques are urgently needed for characterizing the genuine network multipartite entanglement. Finally, it will also be interesting to seek a further extension of the framework in high-order entanglement detection [10] as well as bound entanglement detection.

ACKNOWLEDGMENTS

We thank Yi-Zheng Zhen for very valuable discussion. This work was supported by the National Natural Science Foundation of China (Grants No. 62031024, No. 11874346, and No. 12174375), the National Key R&D Program of China (Grant No. 2019YFA0308700), the Anhui Initiative in Quantum Information Technologies (Grant No. AHY060200), and the Innovation Program for Quantum Science and Technology (Grant No. 2021ZD0301100).

APPENDIX A: PROOF AND DISCUSSIONS OF THE BIPARTITE EW IN EQ. (5)

1. Class of bipartite entanglement witness

Let $|\phi\rangle$ be an arbitrary pure entangled state in the $d \times d$ -dimensional Hilbert space $\mathcal{H}_d \otimes \mathcal{H}_d$. Without loss of generality, we can assume $|\phi\rangle = \sum_{i=0}^{d-1} \sqrt{\lambda_i} |ii\rangle$, where all $\lambda_i \geq 0$

are Schmidt coefficients in decreasing order and $\sum_i \lambda_i = 1$. We can define a positive operator Q as

$$Q = \sum_{\substack{i,j=0 \\ i < j}}^{d-1} \sqrt{\lambda_i \lambda_j} (|ij\rangle - |ji\rangle)(\langle ij| - \langle ji|), \quad (\text{A1})$$

which can be used for constructing an EW for $|\phi\rangle$.

Lemma 1. The partial transpose of Q provides an optimal EW $\mathcal{W}_o^{|\phi\rangle}$, which $\mathcal{W}_o^{|\phi\rangle}$ reads

$$\mathcal{W}_o^{|\phi\rangle} = Q^\Gamma = \sum_{i,j=0}^{d-1} \sqrt{\lambda_i \lambda_j} |ij\rangle \langle ij| - |\phi\rangle \langle \phi|. \quad (\text{A2})$$

Proof. To prove that the $\mathcal{W}_o^{|\phi\rangle}$ is an EW, note that it is of the form Q^Γ with Q being positive-semi-definite ($Q \geq 0$). Thus for all separable states $\text{Tr}(\rho_{\text{sep}} \mathcal{W}_o^{|\phi\rangle}) = \text{Tr}(\rho_{\text{sep}}^\Gamma Q) \geq 0$. Meanwhile, $\text{Tr}(\mathcal{W}_o^{|\phi\rangle} |\phi\rangle \langle \phi|) = \sum_i \lambda_i^2 - 1 = -\sum_{i \neq j} \lambda_i \lambda_j < 0$. Then $\mathcal{W}_o^{|\phi\rangle}$ is an EW by definition.

To show the optimality of $\mathcal{W}_o^{|\phi\rangle}$, it is sufficient to prove that the set of pure separable states $\{|\phi_1\rangle \otimes |\phi_2\rangle\}$ satisfying $\langle \phi_1 | \langle \phi_2 | \mathcal{W}_o^{|\phi\rangle} | \phi_1 \rangle | \phi_2 \rangle = 0$ span the entire Hilbert space $\mathcal{H}_d \otimes \mathcal{H}_d$ [29]. For the qubit case, we have $\mathcal{W}_o^{(2)} = \sqrt{\lambda_0 \lambda_1} (|01\rangle - |10\rangle)(\langle 01| - \langle 10|)^\Gamma$. It is easy to verify that the set of separable states $\{|00\rangle, (|0\rangle + |1\rangle)(|0\rangle + |1\rangle)/2, (|0\rangle + i|1\rangle)(|0\rangle - i|1\rangle)/2, |11\rangle\}$ satisfies $\text{Tr}(\rho_{\text{sep}} \mathcal{W}_o^{(2)}) = 0$. This set of states spans the entire Hilbert space $\mathcal{H}_2 \otimes \mathcal{H}_2$. In fact, it was shown that any decomposable EW acting on $\mathcal{H}_2 \otimes \mathcal{H}_d$ is optimal if and only if it takes the form $\mathcal{W} = Q^\Gamma$ for some $Q \geq 0$ [63].

Similarly, in the qudit case ($d > 2$), there exist separable states $\{|ee\rangle, (|e\rangle + |f\rangle)(|e\rangle + |f\rangle)/2, (|e\rangle + i|f\rangle)(|e\rangle - i|f\rangle)/2, |ff\rangle\}$ satisfying $\text{Tr}(\rho_{\text{sep}} \mathcal{W}_o^{|\phi\rangle}) = 0$, for each pair $0 \leq e < f \leq d-1$. These states span the same space with $\{|ee\rangle, |ef\rangle, |fe\rangle, |ff\rangle\}$. By iterating over all $e < f$, we end up with a set of separable states spanning the entire space $\mathcal{H}_d \otimes \mathcal{H}_d$. Thus the EW $\mathcal{W}_o^{|\phi\rangle}$ is optimal. This finishes the proof. ■

2. Detection of bipartite unfaithful state

Remarkably, for the entangled state $|\phi\rangle$, the most widely used fidelity witness reads $\mathcal{W}_F^{|\phi\rangle} = \lambda_0 I - |\phi\rangle \langle \phi|$. It is straightforward to observe that $\mathcal{W}_F^{|\phi\rangle} - \mathcal{W}_o^{|\phi\rangle} \geq 0$, which means that the $\mathcal{W}_o^{|\phi\rangle}$ is finer than the $\mathcal{W}_F^{|\phi\rangle}$. This leads to a byproduct that the $\mathcal{W}_o^{|\phi\rangle}$ can detect unfaithful states. Unfaithful states are entangled states that cannot be detected by all fidelity witnesses [48], namely, an entangled state ρ is unfaithful if and only if $\text{Tr}(\rho \mathcal{W}_F^{|\psi\rangle}) \geq 0$ for all $|\psi\rangle$. Therefore, the relationship $\mathcal{W}_F^{|\phi\rangle} - \mathcal{W}_o^{|\phi\rangle} \geq 0$ itself is not sufficient to demonstrate that the extra entangled states detected by $\mathcal{W}_o^{|\phi\rangle}$ is unfaithful. A further clarification is required to justify the statement that $\mathcal{W}_o^{|\phi\rangle}$ detects an unfaithful state.

Now we would like to provide qualitative and quantitative characterizations on the ability to detect unfaithfulness of the $\mathcal{W}_o^{|\phi\rangle}$. Consider the class of states $\rho_{|\phi\rangle}(p) = pI/d^2 + (1-p)|\phi\rangle \langle \phi|$. From Observation 1 in Ref. [55], it is known that such states are faithful if and only if they are detected by $\mathcal{W}_m = I/d - |\phi_d^+\rangle \langle \phi_d^+|$, with $|\phi_d^+\rangle$ being the maximally entangled state $\sum_{i=0}^{d-1} 1/\sqrt{d} |ii\rangle$. By solving $\text{Tr}[\rho_{|\phi\rangle}(p) \mathcal{W}_m] = 0$,

TABLE I. Maximal unfaithful length l_d from the class of EWs $\mathcal{W}_o^{|\phi\rangle}$. We remark that the optimization of l_d may arrive at a local maximum. We use enough random starting points to support the claim that we arrive at the global maximum.

| d | 3 | 4 | 5 | 6 | 7 |
|-------|--------|--------|--------|--------|--------|
| l_d | 0.2679 | 0.4202 | 0.5195 | 0.5896 | 0.6624 |

we obtain that the white-noise tolerance of \mathcal{W}_m for $|\phi\rangle$ is

$$p_f^{|\phi\rangle} = \frac{\sum_{i,j=0}^{d-1} \sqrt{\lambda_i \lambda_j} - 1}{\sum_{i,j=0}^{d-1} \sqrt{\lambda_i \lambda_j} - \frac{1}{d}}. \quad (\text{A3})$$

That is, $\rho_{|\phi\rangle}(p)$ is faithful when $p < p_f^{|\phi\rangle}$. Similarly, we can obtain the white-noise tolerance of $\mathcal{W}_o^{|\phi\rangle}$ for $|\phi\rangle$, which is

$$p_o^{|\phi\rangle} = \frac{1 - \sum_{i=0}^{d-1} \lambda_i^2}{1 - \sum_{i=0}^{d-1} \lambda_i^2 + \frac{1}{d^2} (\sum_{i,j=0}^{d-1} \sqrt{\lambda_i \lambda_j} - 1)}. \quad (\text{A4})$$

It can be observed that

$$\begin{aligned} & \frac{1/p_o^{|\phi\rangle} - 1}{1/p_f^{|\phi\rangle} - 1} \\ &= \frac{(\sum_{i,j=0}^{d-1} \sqrt{\lambda_i \lambda_j} - 1)^2}{d(d-1)(1 - \sum_i \lambda_i^2)} \\ &= 1 + \frac{(\sum_{i \neq j} \sqrt{\lambda_i \lambda_j})^2 - d(d-1)(1 - \sum_i \lambda_i^2)}{d(d-1)(1 - \sum_i \lambda_i^2)} \\ &\leq 1 + \frac{d(d-1)(\sum_{i \neq j} \lambda_i \lambda_j) - d(d-1)(1 - \sum_i \lambda_i^2)}{d(d-1)(1 - \sum_i \lambda_i^2)} \\ &= 1 + \frac{d(d-1)[(\sum_{i=0}^{d-1} \lambda_i)^2 - 1]}{d(d-1)(1 - \sum_i \lambda_i^2)} = 1. \end{aligned} \quad (\text{A5})$$

In other words, $p_f^{|\phi\rangle} \leq p_o^{|\phi\rangle}$, where the inequality comes from the Cauchy-Schwarz inequality, and takes equality if $d = 2$ or $\lambda_i = 1/d$ for all i . Therefore, the $\mathcal{W}_o^{|\phi\rangle}$ can always detect an unfaithful state $\rho_{|\phi\rangle}(p)$ for $p \in [p_f^{|\phi\rangle}, p_o^{|\phi\rangle})$, unless $|\phi\rangle$ is a two-qubit state or maximally entangled.

As a quantitative investigation, we numerically maximize the interval length l_d of $[p_f^{|\phi\rangle}, p_o^{|\phi\rangle})$ over all $|\phi\rangle$ for different local dimension d . We name l_d the maximal unfaithful length from the class of EWs $\mathcal{W}_o^{|\phi\rangle}$ and the results are listed in Table I for $d = 3, 4, \dots, 7$. It can be seen that l_d grows significantly with an increasing dimension d , indicating that the $\mathcal{W}_o^{|\phi\rangle}$ can greatly outperform the fidelity witness. This is also in agreement with the statement that most states are unfaithful as claimed in Ref. [48].

Except for the l_d , one may be also interested in the average performance of this different class of EWs on unfaithfulness detection. As a comparison, it is natural to consider two intervals $[p_e^{|\phi\rangle}, p_f^{|\phi\rangle})$ and $[p_o^{|\phi\rangle}, p_f^{|\phi\rangle})$, where the $p_e^{|\phi\rangle}$ is the critical value such that $\rho_{|\phi\rangle}(p)$ becomes separable. The first interval contains all unfaithful $\rho_{|\phi\rangle}(p)$, while the second contains the part that can be detected by the class of $\mathcal{W}_o^{|\phi\rangle}$. Then we can use $\text{avg}_{|\phi\rangle}(p_o^{|\phi\rangle} - p_f^{|\phi\rangle}) / (p_e^{|\phi\rangle} - p_f^{|\phi\rangle})$ to evaluate the average

TABLE II. Average performance of $\mathcal{W}_o^{|\phi\rangle}$ for detecting unfaithfulness. For different local dimension d , the average is taken by randomly generating 10^7 pure states in $\mathcal{H}_d \otimes \mathcal{H}_d$. Since any pure bipartite state admits a Schmidt decomposition $|\phi\rangle = \sum_i \sqrt{\lambda_i} |ii\rangle$, we replace the randomly generated pure bipartite states with random vectors $(\sqrt{\lambda_0}, \dots, \sqrt{\lambda_{d-1}})$ uniformly distributed on the d -dimensional unit sphere. Moreover, the critical value $p_e^{|\phi\rangle}$ is $\frac{d^2 \sqrt{\lambda_0 \lambda_1}}{1 + d^2 \sqrt{\lambda_0 \lambda_1}}$ according to the results in Ref. [64], assuming that the Schmidt coefficients λ_i are in decreasing order.

| d | 3 | 4 | 5 | 6 | 7 |
|---|--------|--------|--------|--------|--------|
| $\text{avg}_{ \phi\rangle}(p_o^{ \phi\rangle} - p_f^{ \phi\rangle})$ | 0.0804 | 0.0969 | 0.0963 | 0.0909 | 0.0848 |
| $\text{avg}_{ \phi\rangle}(p_e^{ \phi\rangle} - p_f^{ \phi\rangle})$ | 0.1190 | 0.1460 | 0.1457 | 0.1379 | 0.1286 |
| $\text{avg}_{ \phi\rangle} \frac{p_o^{ \phi\rangle} - p_f^{ \phi\rangle}}{p_e^{ \phi\rangle} - p_f^{ \phi\rangle}}$ | 0.5605 | 0.5937 | 0.6089 | 0.6181 | 0.6248 |

performance of $\mathcal{W}_o^{|\phi\rangle}$ for detecting unfaithfulness, as shown in Table II. It is observed that a large percentage of unfaithful states are detected. This is also the premise that GME witnesses constructed from this class of bipartite EWs can detect a multipartite unfaithful state.

3. Generalization of Lemma 1

Finally, we provide a generalization of Lemma 1. For the above entangled state $|\phi\rangle$, we can construct another positive operator

$$\tilde{Q} = \sum_{\substack{i,j=0 \\ i < j}}^{d-1} (\alpha_{ij}|ij\rangle - \beta_{ij}|ji\rangle)(\alpha_{ij}\langle ij| - \beta_{ij}\langle ji|), \quad (\text{A6})$$

instead of Q , where $\alpha_{ij}\beta_{ij} = \sqrt{\lambda_i \lambda_j}$ and α_{ij}, β_{ij} are all positive. The operator $\tilde{\mathcal{W}}_o = \tilde{Q}^\Gamma$ is also optimal EW and applicable in our framework for GME witness construction. Here, the proof of the optimality of $\tilde{\mathcal{W}}_o$ is similar to the case in Lemma 1. It is sufficient to verify that the set of states $\{|ee\rangle, |ff\rangle, (\sqrt{\beta_{ef}}|e\rangle + \sqrt{\alpha_{ef}}|f\rangle) \otimes (\sqrt{\alpha_{ef}}|e\rangle + \sqrt{\beta_{ef}}|f\rangle), (\sqrt{\beta_{ef}}|e\rangle + i\sqrt{\alpha_{ef}}|f\rangle) \otimes (\sqrt{\alpha_{ef}}|e\rangle - i\sqrt{\beta_{ef}}|f\rangle)\}_{e,f=0}^{d-1}$ have zero expectation value when measured with $\tilde{\mathcal{W}}_o$ and span the entire d^2 -dimensional Hilbert space.

APPENDIX B: PROOF OF THE EXAMPLES

In this section, we will show explicitly how this construction can be applied to some commonly used multipartite entangled states and make further discussions on the results.

1. W state

The W state is an important class of multiqubit entangled states. A class of EWs for the W state which can outperform significantly than the fidelity witness was proposed in Ref. [51]. In Ref. [51], the authors constructed an operator at first and then proved that this operator was a decomposable bipartite EW with respect to all possible bipartitions. Contrarily, our construction is in the opposite direction. We construct a complete set of bipartite EWs for the W state and lift them

to a GME witness. Although different methods were used, our construction recovers the result in Ref. [51].

We start with the simplest three-qubit case, where the target state is

$$|W_3\rangle = \frac{1}{\sqrt{3}}(|001\rangle + |010\rangle + |100\rangle). \quad (\text{B1})$$

For the bipartition $1|23$, the EW constructed from Lemma 1 is of the form

$$\begin{aligned} \mathcal{W}_{1|23}^{W_3} &= \frac{\sqrt{2}}{3}(|000\rangle\langle 000| + |1\psi^+\rangle\langle 1\psi^+|) \\ &+ \frac{2}{3}|0\psi^+\rangle\langle 0\psi^+| + \frac{1}{3}|100\rangle\langle 100| - |W_3\rangle\langle W_3|, \end{aligned} \quad (\text{B2})$$

with $|\psi^+\rangle = (|01\rangle + |10\rangle)/\sqrt{2}$. For the other two bipartitions, the $\mathcal{W}_{2|13}$ and $\mathcal{W}_{3|12}$ can be obtained after a permutation of the qubits. Then for $|W_3\rangle$, the set \mathcal{S} reads

$$\begin{aligned} \mathcal{S} &= \{|000\rangle\langle 000|, |001\rangle\langle 001|, |010\rangle\langle 010|, |100\rangle\langle 100|, \\ &|0\psi^+\rangle\langle 0\psi^+|, |0_2\psi_{13}^+\rangle\langle 0_2\psi_{13}^+|, |\psi^+0\rangle\langle \psi^+0|, \\ &|1\psi^+\rangle\langle 1\psi^+|, |1_2\psi_{13}^+\rangle\langle 1_2\psi_{13}^+|, |\psi^+1\rangle\langle \psi^+1|\}. \end{aligned} \quad (\text{B3})$$

These states in \mathcal{S} can be grouped into three subsets according to the procedure in the main text:

$$\begin{aligned} \mathcal{S}_1 &= \{|000\rangle\langle 000|\}, \\ \mathcal{S}_2 &= \{|001\rangle\langle 001|, |010\rangle\langle 010|, |100\rangle\langle 100|, \\ &|0\psi^+\rangle\langle 0\psi^+|, |0_2\psi_{13}^+\rangle\langle 0_2\psi_{13}^+|, |\psi^+0\rangle\langle \psi^+0|\}, \\ \mathcal{S}_3 &= \{|1\psi^+\rangle\langle 1\psi^+|, |1_2\psi_{13}^+\rangle\langle 1_2\psi_{13}^+|, |\psi^+1\rangle\langle \psi^+1|\}, \end{aligned} \quad (\text{B4})$$

and the corresponding α_k by Theorem 1 is

$$\alpha_1 = \sqrt{2}/3, \quad \alpha_2 = 2/3, \quad \alpha_3 = \sqrt{2}/3, \quad (\text{B5})$$

respectively. This result in a GME witness

$$\begin{aligned} \mathcal{W}_{|W_3} &= \frac{\sqrt{2}}{3}(|000\rangle\langle 000| + |101\rangle\langle 101| + |011\rangle\langle 011| \\ &+ |110\rangle\langle 110|) + \frac{2}{3}(|001\rangle\langle 001| + |010\rangle\langle 010| \\ &+ |100\rangle\langle 100|) - |W_3\rangle\langle W_3|. \end{aligned} \quad (\text{B6})$$

Moreover, by employing the generalization of Lemma 1 in Eq. (A6), we obtain

$$\mathcal{W}'_{1|23} = [(a|0\rangle\langle 00| - b|1\rangle\langle \psi^+|)(a\langle 0|\langle 00| - b\langle 1|\langle \psi^+|)]^{\Gamma_1}, \quad (\text{B7})$$

where a, b are positive numbers and satisfy $ab = \sqrt{2}/3$. The other two bipartite EWs are obtained immediately after rearrangement of the qubits. For this set of bipartite EWs, the EW $\mathcal{W}_{|W_3}$ can be generalized into

$$\begin{aligned} \mathcal{W}'_{|W_3} &= a^2|000\rangle\langle 000| + b^2(|101\rangle\langle 101| + |011\rangle\langle 011| \\ &+ |110\rangle\langle 110|) + \frac{2}{3}(|001\rangle\langle 001| + |010\rangle\langle 010| \\ &+ |100\rangle\langle 100|) - |W_3\rangle\langle W_3|. \end{aligned} \quad (\text{B8})$$

In n -qubit cases, if a subsystem A contains m qubits, the corresponding bipartite EW from Lemma 1 is of the form ($1 \leq m \leq n-1$)

$$\mathcal{W}_{m|n-m} = \sqrt{\frac{m(n-m)}{n^2}} |\psi\rangle_{m|n-m} \langle \psi|^{\Gamma_A}, \quad (\text{B9})$$

where $|\psi\rangle_{m|n-m} = |0\rangle_A^{\otimes m} |0\rangle_{\bar{A}}^{\otimes n-m} - |W_m\rangle_A |W_{n-m}\rangle_{\bar{A}}$. Then the set \mathcal{S} for $|W_n\rangle$ can still be grouped into three subsets

$$\{|0^{\otimes n}\rangle\}, \{|\pi_m(0^{\otimes n-1}1)\rangle\}, \{|\pi'_m(0^{\otimes n-2}1^{\otimes 2})\rangle\}, \quad (\text{B10})$$

with the corresponding coefficients α_k being

$$\begin{aligned} \alpha_1 &= \max_m \sqrt{\frac{m(n-m)}{n^2}} = \frac{\sqrt{[n/2](n-[n/2])}}{n}, \\ \alpha_2 &= \max_m \frac{n-m}{n} = \frac{n-1}{n}, \\ \alpha_3 &= \max_m \sqrt{\frac{m(n-m)}{n^2}} = \frac{\sqrt{[n/2](n-[n/2])}}{n}. \end{aligned} \quad (\text{B11})$$

Therefore we arrive at the following $\mathcal{W}_{|W_n}$:

$$\begin{aligned} \mathcal{W}_{|W_n} &= \frac{n-1}{n} \mathcal{P}_1 + \frac{\sqrt{[n/2](n-[n/2])}}{n} (|0\rangle\langle 0|^{\otimes n} + \mathcal{P}_2) \\ &- |W_n\rangle\langle W_n|, \end{aligned} \quad (\text{B12})$$

with $\mathcal{P}_i = \sum_m \pi_m (|0\rangle^{\otimes n-i} |1\rangle^{\otimes i}) \pi_m (\langle 0|^{\otimes n-i} \langle 1|^{\otimes i})$, where the summation m is over all possible permutations of $|0\rangle^{\otimes n-i} |1\rangle^{\otimes i}$.

The EW $\mathcal{W}_{|W_n}$ can also be generalized in a similar manner with the $\mathcal{W}_{|W_3}$ so as to recover the results of Ref. [51]. Although ending up with the same witness operator, our construction provides a different insight on why the $\mathcal{W}_{|W_n}$ takes such a form.

2. Graph states

Before discussing the construction of GME witnesses for the graph states, we first give a brief introduction to the graph states. A graph is a pair $G = (V, E)$ of sets where the elements of V are called vertices and the elements of E are edges connecting the vertices. For example, $(1, 2)$ represents the edge connecting vertex 1 and 2. Two vertices are called neighboring if they are connected by an edge. A graph can also be represented by the adjacency matrix Γ with

$$\Gamma_{ij} = \begin{cases} 1, & \text{if } (v_i, v_j) \in E, \\ 0, & \text{otherwise.} \end{cases} \quad (\text{B13})$$

Then, an n -qubit graph state $|G\rangle$ is defined with an n -vertex graph G whose vertices correspond to qubits and edges correspond to control-Z (CZ) gate between two qubits. The graph state can be expressed with a set of stabilizers

$$g_i = X_i \prod_{j \in N(i)} Z_j, \quad i = 1, \dots, n, \quad (\text{B14})$$

where X_i and Z_i are the Pauli operators on qubit (vertex) i , and $N(i)$ is the neighborhood of i (i.e., the set of vertices directly connected to i by edges). These operators g_i commute with each other and $|G\rangle$ is the common eigenstate of them such that

$$\forall i = 1, \dots, n, \quad g_i |G\rangle = |G\rangle. \quad (\text{B15})$$

Moreover, all the 2^n common eigenstates of these g_i form a basis named a graph-state basis. Each term in this basis is uniquely decided by the eigenvalues of g_i . As the eigenvalues of g_i are either 1 or -1 , the graph-state basis can be denoted by a vector $\vec{a} \in \{0, 1\}^n$ such that

$$\forall i = 1, \dots, n, \quad g_i |a_1 \cdots a_n\rangle_G = (-1)^{a_i} |a_1 \cdots a_n\rangle_G. \quad (\text{B16})$$

The density matrix of $|\vec{a}\rangle_G$ is

$$|a_1 \cdots a_n\rangle_G \langle a_1 \cdots a_n| = \prod_{i=1}^n \frac{(-1)^{a_i} g_i + I}{2}. \quad (\text{B17})$$

Specifically, the graph state $|G\rangle$ is denoted as $|0 \cdots 0\rangle_G$.

Remarkably, by choosing the graph-state basis instead of the computational basis, the calculation of GME witness construction can be greatly simplified without needing to perform the Schmidt decomposition. First, the partial transposition of a graph state is diagonal under the graph-state basis, namely, $|\vec{a}_0\rangle_G \langle \vec{a}_0|^T$ is of the form $\sum_{\vec{a}} c_{\vec{a}} |\vec{a}\rangle_G \langle \vec{a}|$. Meanwhile, the operator \mathcal{Q} in Eq. (A1) can be seen as a linear combination of all the eigenstates with a negative eigenvalue of $|G\rangle \langle G|^T$. Therefore, when Lemma 1 is applied to the graph state $|G\rangle$, the resulting bipartite EW $\mathcal{W}_{o, A|\bar{A}}^{(G)}$ is diagonal in the graph-state basis. In this case, the vectors in the set \mathcal{S} can be taken as the base vectors $|\vec{a}\rangle_G$, such that the construction in Theorem 1 is easy to achieve. In the following, we propose an explicit procedure for finding the decomposition of $\mathcal{W}_{o, A|\bar{A}}^{(G)}$ in the graph-state basis.

First, for the given bipartition $A|\bar{A}$, the adjacency matrix Γ can be decomposed into the following blocks:

$$\begin{pmatrix} G_A & \Gamma_{A|\bar{A}} \\ \Gamma_{A|\bar{A}} & G_{\bar{A}} \end{pmatrix}. \quad (\text{B18})$$

We denote $k = \text{rank}(\Gamma_{A|\bar{A}})$ as the rank of the submatrix $\Gamma_{A|\bar{A}}$. It is known that a graph state can be transformed into tensor product of k Bell states across the partitions A and \bar{A} , using CZ gates within each partition and local complementation operations [42]. Here the local complementation τ_a on a vertex a is defined as follows: $\tau_a : G \rightarrow \tau_a(G)$, such that the edge set E' of the new graph $\tau_a(G)$ is $E' = E \cup E[N(a), N(a)] - E \cap E[N(a), N(a)]$. The local complementation $\tau_a(G)$ can be implemented with the following local unitary operation [42]:

$$U_a(G) = (-iX_a)^{1/2} \prod_{b \in N(a)} (iZ_b)^{1/2}. \quad (\text{B19})$$

After this operation, $|G\rangle$ is turned into $|\tau_a(G)\rangle$ and the stabilizers of $|G\rangle$ transform according to the following equations:

$$\begin{aligned} U_a(G) g_b^G U_a(G) &= g_a^{\tau_a(G)} g_b^{\tau_a(G)}, & \text{if } b \in N(a); \\ U_a(G) g_b^G U_a(G) &= g_b^{\tau_a(G)}, & \text{if } b \notin N(a). \end{aligned} \quad (\text{B20})$$

Meanwhile, we remark that a bipartite EW $\mathcal{W}_{A|\bar{A}}$ for $|G\rangle$ is transformed into another bipartite EW $\mathcal{W}'_{A|\bar{A}}$ for $|G'\rangle$ after some local unitary operation with respect to $A|\bar{A}$. Hence our task for constructing bipartite EW of the initial graph state $|G\rangle$ is turned into finding a bipartite EW for $|\text{Bell}\rangle^{\otimes k}$ by employing Lemma 1; a much easier task compared with the initial one.

Second, after reversing the above transformation process from $|G\rangle$ to $|\text{Bell}\rangle^{\otimes k}$, the EW for $|\text{Bell}\rangle^{\otimes k}$ which is diagonal in the Bell-state basis will be turned back into a bipartite EW

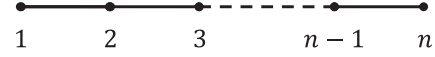


FIG. 4. Representation of n -qubit linear cluster state with graph, where n qubits are connected one by one with CZ gates.

for $|G\rangle$ which is diagonal in graph-state basis. With the above foundation, we move on to an explicit discussion on a typical class of graph states: the linear cluster state $|\text{Cl}_n\rangle$. The linear cluster state is represented with the graph in Fig. 4.

We call the bipartition $A|\bar{A}$ a rank- k bipartition if $\text{rank}(\Gamma_{A|\bar{A}}) = k$, with the $\Gamma_{A|\bar{A}}$ defined in Eq. (B18). All rank-1 bipartitions of the linear cluster state have only two possible types of the subgraph on the boundary $\Gamma_{A|\bar{A}}$ (Fig. 5). Any other edge is deleted by CZ gates within each partition. For the type-1 subgraph $G_{i,i+1}$, the bipartite EW reads

$$\begin{aligned} \mathcal{W}_{G_{i,i+1}} &= \frac{1}{2} (|0_i 0_{i+1}\rangle_{G_{i,i+1}} \langle 0_i 0_{i+1}| + |0_i 1_{i+1}\rangle_{G_{i,i+1}} \langle 0_i 1_{i+1}| \\ &\quad + |1_i 0_{i+1}\rangle_{G_{i,i+1}} \langle 1_i 0_{i+1}| + |1_i 1_{i+1}\rangle_{G_{i,i+1}} \langle 1_i 1_{i+1}|) \\ &\quad - |G_{i,i+1}\rangle \langle G_{i,i+1}|, \end{aligned} \quad (\text{B21})$$

by employing Lemma 1, where the state vectors like $|0_i 1_{i+1}\rangle_{G_{i,i+1}}$ are graph-state basis-defined in Eq. (B16), and the “0”s on the other vertices are omitted for simplicity here and after. Note that the $g_j^{G_{i,i+1}}$ can be transformed back to the $g_j^{\text{Cl}_n}$ by employing CZ gates without disturbing the eigenvalue of the state vector. Therefore, the bipartite EW for the original state $|\text{Cl}_n\rangle$ is

$$\begin{aligned} \mathcal{W}_{A|\bar{A}} &= \frac{1}{2} (|\text{Cl}_n\rangle \langle \text{Cl}_n| + |0_i 1_{i+1}\rangle_{\text{Cl}_n} \langle 0_i 1_{i+1}| \\ &\quad + |1_i 0_{i+1}\rangle_{\text{Cl}_n} \langle 1_i 0_{i+1}| + |1_i 1_{i+1}\rangle_{\text{Cl}_n} \langle 1_i 1_{i+1}|) \\ &\quad - |\text{Cl}_n\rangle \langle \text{Cl}_n|, \end{aligned} \quad (\text{B22})$$

when formulated in the graph-state basis. After normalizing the $\mathcal{W}_{A|\bar{A}}$ to meet the constraint $\text{Tr}(\mathcal{W}_{A|\bar{A}} |\text{Cl}_n\rangle \langle \text{Cl}_n|) = -1$, we obtain

$$\begin{aligned} \mathcal{W}'_{A|\bar{A}} &= |0_i 1_{i+1}\rangle_{\text{Cl}_n} \langle 0_i 1_{i+1}| + |1_i 0_{i+1}\rangle_{\text{Cl}_n} \langle 1_i 0_{i+1}| \\ &\quad + |1_i 1_{i+1}\rangle_{\text{Cl}_n} \langle 1_i 1_{i+1}| - |\text{Cl}_n\rangle \langle \text{Cl}_n|, \end{aligned} \quad (\text{B23})$$

as the bipartite EW used in our construction. This bipartite EW contributes the following terms to the set \mathcal{S} :

$$\{|0_i 1_{i+1}\rangle_{\text{Cl}_n}, |1_i 0_{i+1}\rangle_{\text{Cl}_n}, |1_i 1_{i+1}\rangle_{\text{Cl}_n}\}. \quad (\text{B24})$$

This set is denoted as $\mathcal{S}_{i, \text{type}1} = \{01, 10, 11\}_{i, i+1}$ for short.

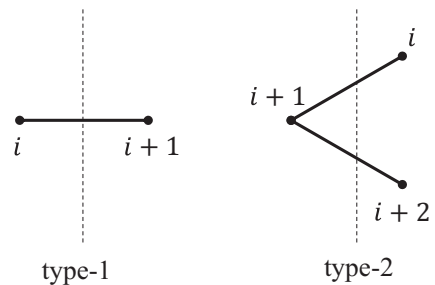


FIG. 5. Possible subgraphs on the boundary across rank-1 bipartition. For a given bipartition $A|\bar{A}$, if $\text{rank}(\Gamma_{A|\bar{A}}) = 1$, then the subgraph across this bipartition has only the above two types.

Meanwhile, the type-2 subgraph $G_{i,i+1,i+2}$ in Fig. 5 can be transformed into the type-1 subgraph after applying $C_{Z,(i,i+2)}$, $U_i(G_{i,i+1,i+2})$, and $C_{Z,(i,i+2)}$ sequentially. We remark that the local complementation operation $U_i(G_{i,i+1,i+2})$ may change the corresponding eigenvalue when $g_j^{G_{i,i+1,i+2}}$ turns into $g_j^{G_{i,i+1}}$, which is decided by Eq. (B20). Therefore, these kinds of bipartitions contribute the following set of states to the set \mathcal{S} :

$$\mathcal{S}_{i,\text{type}2} = \{010, 101, 111\}_{i,i+1,i+2}. \quad (\text{B25})$$

In summary, all the rank-1 bipartitions contribute an operator R_1 by our construction. If we denote the V_1 as the set of vectors from $\{0, 1\}^n$ such that the maximal distance between the “1”s appearing in each vector is smaller than 3, the R_1 can be formulated as

$$R_1 = \sum_{\vec{a} \in V_1} |\vec{a}\rangle_{\text{Cl}_n} \langle \vec{a}|. \quad (\text{B26})$$

For rank-2 bipartitions, their boundaries are composed of two rank-1 boundaries. For example, if there are two type-1 parts, the bipartite EW takes the form

$$\mathcal{W}_{A|\bar{A}} = \frac{1}{4} \sum_{\vec{a} \in \{0,1\}^4} |\vec{a}_{i,i+1,j,j+1}\rangle_{\text{Cl}_n} \langle \vec{a}_{i,i+1,j,j+1}| - |\text{Cl}_n\rangle \langle \text{Cl}_n|. \quad (\text{B27})$$

After normalization, the bipartite EW reads

$$\mathcal{W}_{A|\bar{A}} = \frac{1}{3} \sum_{\substack{\vec{a} \in \{0,1\}^4, \\ \vec{a} \neq \vec{0}}} |\vec{a}_{i,i+1,j,j+1}\rangle_{\text{Cl}_n} \langle \vec{a}_{i,i+1,j,j+1}| - |\text{Cl}_n\rangle \langle \text{Cl}_n|. \quad (\text{B28})$$

Such a bipartite EW contributes the following new terms to the set \mathcal{S} :

$$\mathcal{S}_{i,\text{type}1} \otimes \mathcal{S}_{j,\text{type}1} = \{0101, 0110, 0111, 1001, 1010, 1011, 1101, 1110, 1111\}_{i,i+1,j,j+1}. \quad (\text{B29})$$

The contribution of other possibilities can be decided in a similar manner as above for the type-2 subgraph. All these rank-2 bipartitions contribute a set V_2 to \mathcal{S} . Here a vector from $\{0, 1\}^n$ belongs to V_2 if there exist at most two “1”s whose distance is larger than 2 at the same time in the vector. Finally, all the rank-2 bipartitions introduce an operator R_2 to our construction, with

$$R_2 = \sum_{\vec{a} \in V_2} \frac{1}{3} |\vec{a}\rangle_{\text{Cl}_n} \langle \vec{a}|. \quad (\text{B30})$$

For a rank- k bipartition, the subgraph on the boundary is nothing but a combination of k rank-1 part. After repeating the above process, it is shown that all the rank- k bipartitions contribute the following operator R_k :

$$R_k = \sum_{\vec{a} \in V_k} \frac{1}{2^k - 1} |\vec{a}\rangle_{\text{Cl}_n} \langle \vec{a}|. \quad (\text{B31})$$

A vector \vec{a} belongs to V_k if there exist at most k for the number of “1”s in \vec{a} , such that their distance with each other are larger than k at the same time. It can be observed immediately that $k \leq \lceil n/3 \rceil$, indicating that the partition whose rank is higher than $\lceil n/3 \rceil$ gives no extra contribution.

After considering all the bipartitions, we end up with the GME witness $\mathcal{W}_{\text{Cl}_n}$ introduced in the main text, namely,

$$\mathcal{W}_{\text{Cl}_n} = \sum_{k=1}^{\lceil n/3 \rceil} R_k - |\text{Cl}_n\rangle \langle \text{Cl}_n|. \quad (\text{B32})$$

As an example, for the four-qubit cluster state

$$\mathcal{W}_{\text{Cl}_4} = \sum_{\vec{a} \in V_1} |\vec{a}\rangle_G \langle \vec{a}| + \frac{1}{3} \sum_{\vec{a} \in V_2} |\vec{a}\rangle_G \langle \vec{a}| - |G\rangle \langle G|, \quad (\text{B33})$$

where V_1 is the set $\{0001, 0010, 0011, 0100, 0101, 0110, 0111, 1000, 1010, 1100, 1110\}$, and V_2 is the set $\{1001, 1011, 1101, 1111\}$.

Remarkably, in the four-qubit case, the best-known EW is [45]

$$\mathcal{W}_{\text{Cl}_4}^{\text{opt}} = \sum_{\vec{a} \in V_1} |\vec{a}\rangle_G \langle \vec{a}| - |G\rangle \langle G|. \quad (\text{B34})$$

It is finer than the $\mathcal{W}_{\text{Cl}_4}$ above. That is, while our approach is already quite powerful, there is still room for improvement. In this particular case, the improvement can be achieved by an elaborate choice of the set of bipartite EWs, instead of using Lemma 1 only. If the bipartite EWs for 13|24 and 14|23 in the above construction are replaced by

$$\begin{aligned} \mathcal{W}_{13|24} &= |0001\rangle_{\text{Cl}_4} \langle 0001| + |0100\rangle_{\text{Cl}_4} \langle 0100| \\ &\quad + |0101\rangle_{\text{Cl}_4} \langle 0101| + |0011\rangle_{\text{Cl}_4} \langle 0011| \\ &\quad + |0110\rangle_{\text{Cl}_4} \langle 0110| + |0111\rangle_{\text{Cl}_4} \langle 0111| - |\text{Cl}_4\rangle \langle \text{Cl}_4|, \\ \mathcal{W}_{14|23} &= |0001\rangle_{\text{Cl}_4} \langle 0001| + |0010\rangle_{\text{Cl}_4} \langle 0010| \\ &\quad + |0101\rangle_{\text{Cl}_4} \langle 0101| + |0011\rangle_{\text{Cl}_4} \langle 0011| \\ &\quad + |0110\rangle_{\text{Cl}_4} \langle 0110| + |0111\rangle_{\text{Cl}_4} \langle 0111| - |\text{Cl}_4\rangle \langle \text{Cl}_4|, \end{aligned} \quad (\text{B35})$$

respectively, we can recover the $\mathcal{W}_{\text{Cl}_4}^{\text{opt}}$ with Theorem 1. With this example on the four-qubit cluster state, we highlight that Lemma 1 is just an alternative choice which ends up with robust GME witnesses. Our construction, in fact, allows a flexible choice on the set of EWs to be lifted to the multipartite case, and a suitable choice can further improve its performance. Moreover, it should be remarked that our discussion was based on the partial transposition throughout this paper to obtain higher noise resistance. If bipartite EWs in the construction are designed by other positive maps (e.g., the Choi’s map), different classes of GME witness can be found. This may help to harness the full potential of Theorem 1 in future work.

3. Multipartite states admitting Schmidt decomposition

A special case of multipartite entangled states is the multipartite states admitting Schmidt decomposition. Without loss of generality, we can assume that such states are of the form $|\phi_s\rangle = \sum_{i=0}^{d-1} \sqrt{\lambda_i} |i\rangle^{\otimes n}$ with $\lambda_i \geq 0$ in decreasing order. Then

Lemma 1 gives a set of bipartite EWs $\mathcal{W}_{A|\bar{A}}^{|\phi_{SD}\rangle}$:

$$\mathcal{W}_{A|\bar{A}}^{|\phi_{SD}\rangle} = \sum_{i,j=0}^{d-1} \sqrt{\lambda_i \lambda_j} |i\rangle_A^{\otimes k} |j\rangle_{\bar{A}}^{\otimes n-k} \langle i|^{\otimes k} \langle j|^{\otimes n-k} - |\phi_s\rangle \langle \phi_s|, \quad (\text{B36})$$

where $k = |A|$ is the number of qudits in subsystem A . For these bipartite EWs, the set S is

$$\{\pi_m(|i\rangle^{\otimes r} |j\rangle^{\otimes n-r})\}_{r,i,j,\pi_m} \cup \{|l\rangle^{\otimes n}\}_{l=0}^{d-1}, \quad (\text{B37})$$

with $r = 1, 2, \dots, n-1$, $i, j = 0, 1, \dots, d-1$ ($i < j$) and π_m being all possible permutations of $|i\rangle^{\otimes r} |j\rangle^{\otimes n-r}$. Note that all state vectors in S are orthogonal with each other, thus our construction ends up with the following multipartite EW:

$$\begin{aligned} \mathcal{W}_{|\phi_s\rangle} &= \sum_{\substack{i,j=0 \\ i < j}}^{d-1} \sum_{r=1}^{n-1} \sum_m \sqrt{\lambda_i \lambda_j} \pi_m(|i\rangle^{\otimes r} |j\rangle^{\otimes n-r}) \pi_m(\langle i|^{\otimes r} \langle j|^{\otimes n-r}) \\ &+ \sum_{i=0}^{d-1} \lambda_i |i\rangle^{\otimes n} \langle i|^{\otimes n} - |\phi_s\rangle \langle \phi_s|, \end{aligned} \quad (\text{B38})$$

where the summation of m is over all possible permutations $\pi_m(|i\rangle^{\otimes r} |j\rangle^{\otimes n-r})$ of $|i\rangle^{\otimes r} |j\rangle^{\otimes n-r}$.

Moreover, similar to the case of proving the optimality of $\mathcal{W}_o^{|\phi\rangle}$ in the first section, we can verify the optimality of $\mathcal{W}_{|\phi_s\rangle}$ by checking that all the biseparable states satisfying $\text{Tr}(\mathcal{W}_{|\phi_s\rangle} \rho_{bs}) = 0$ span the entire Hilbert space $\mathcal{H}_d^{\otimes n}$.

For the special case of n -qudit GHZ states, the white-noise tolerance of $\mathcal{W}_{|\text{GHZ}_n^d\rangle}$ is $\frac{d^{n-1}}{d^{n-1} + 2^{n-1} - 1}$ and converges to 1 for large n as long as $d > 2$. It is also noted that in Ref. [50], a slightly lower bound $\frac{d^{n-1}}{d^{n-1} + 2^{n-1} - 1 + \frac{1}{d-2}}$ was obtained by the construction of multipartite nonpositive map that were positive on the subset of biseparable states. However, such a map and $\mathcal{W}_{|\text{GHZ}_n^d\rangle}$ detects fairly different class of GME states, although they have similar performance under white noise.

4. GME witness for multiqubit singlet states

Multiqubit singlet states are of particular experimental interest, while the GME witness for them is less investigated. In this example, it is shown that our framework works well for the multi-qubit singlet states. In the main text, we provide the result for a specific class of four-qubit singlet states. However, here we begin with the discussion on general four-qubit singlet states

$$|\varphi_4\rangle = a|\psi_{12}^-\rangle \otimes |\psi_{34}^-\rangle + e^{i\theta} b|\psi_{13}^-\rangle \otimes |\psi_{24}^-\rangle, \quad (\text{B39})$$

with the constraint $a^2 + b^2 + \cos(\theta)ab = 1$ and $|\psi_{12}^-\rangle$ being the two-qubit singlet state $(|01\rangle - |10\rangle)/\sqrt{2}$ on the first two qubits. By performing our construction procedure for all four-qubit singlet states, it is observed that the set \mathcal{S} is always divided into five subsets and the identity operators on the corresponding subspaces are just $\{\mathcal{P}_i^4\}_{i=0}^4$ [the \mathcal{P}_i^4 is defined below Eq. (B12)]. More specifically, the resulting witness is

$$\mathcal{W}_4 = c_2 \mathcal{P}_2^4 + c_1 (\mathcal{P}_1^4 + \mathcal{P}_3^4) + c_0 (\mathcal{P}_0^4 + \mathcal{P}_4^4) - |\varphi_4\rangle \langle \varphi_4|, \quad (\text{B40})$$

with the coefficients decided by

$$\begin{aligned} c_2 &= \max \left\{ 1 - \frac{3}{4}a^2, 1 - \frac{3}{4}b^2, \frac{3}{4}(a^2 + b^2) - \frac{1}{2} \right\}, \\ c_1 &= \frac{1}{2}, \\ c_0 &= \max \left\{ \frac{1}{2} - \frac{1}{4}(a^2 + b^2), \frac{1}{4}a^2, \frac{1}{4}b^2 \right\}. \end{aligned} \quad (\text{B41})$$

Specifically, with a choice of $\theta = \pi/2$, this recovers the EW in the main text. While if $a = -1$, $b = 1$, and $\theta = 0$, $|\varphi_4\rangle$ becomes a biseparable state $|\psi_{14}^-\rangle \otimes |\psi_{23}^-\rangle$ and the corresponding EW becomes positive-semi-definite.

When the number of qubit grows, achieving a general expression becomes more complicated. To investigate the GME witness construction in this case, we consider the following six-qubit singlet state:

$$\begin{aligned} |\varphi_6\rangle &= \frac{1}{2} (|\psi_{12}^-\rangle \otimes |\psi_{34}^-\rangle \otimes |\psi_{56}^-\rangle + i|\psi_{13}^-\rangle \otimes |\psi_{24}^-\rangle \otimes |\psi_{56}^-\rangle \\ &+ i|\psi_{12}^-\rangle \otimes |\psi_{35}^-\rangle \otimes |\psi_{46}^-\rangle - |\psi_{13}^-\rangle \otimes |\psi_{25}^-\rangle \otimes |\psi_{46}^-\rangle), \end{aligned} \quad (\text{B42})$$

for which we arrive at the GME witness

$$\begin{aligned} \mathcal{W}_6 &= \frac{5}{8} \mathcal{P}_3^6 + \frac{1}{2} (\mathcal{P}_2^6 + \mathcal{P}_4^6) + \frac{1}{4} (\mathcal{P}_1^6 + \mathcal{P}_5^6) \\ &+ \frac{1}{8} (\mathcal{P}_0^6 + \mathcal{P}_6^6) - |\varphi_6\rangle \langle \varphi_6|. \end{aligned} \quad (\text{B43})$$

Based on these results, it is reasonable to conjecture that for some $2n$ -qubit singlet state $|\varphi_{2n}\rangle$, there exists a GME witness taking the form

$$\mathcal{W}_{2n} = c_n \mathcal{P}_n^{2n} + \sum_{i=0}^{n-1} c_i (\mathcal{P}_i^{2n} + \mathcal{P}_{2n-i}^{2n}) - |\varphi_{2n}\rangle \langle \varphi_{2n}|, \quad (\text{B44})$$

with $c_i \geq c_{i-1} \geq 0$ for $i = 1, \dots, n$ and c_n is the maximal squared overlap between $|\varphi_6\rangle$ and biseparable states. Moreover, if c_i scales with $(1/2)^{-(n-i+1)}$ as in the four- and six-qubit case, a high white-noise tolerance tending to 1 can be expected for a large number of qubits.

[1] R. Horodecki, P. Horodecki, M. Horodecki, and K. Horodecki, Quantum entanglement, *Rev. Mod. Phys.* **81**, 865 (2009).
 [2] E. Chitambar and G. Gour, Quantum resource theories, *Rev. Mod. Phys.* **91**, 025001 (2019).
 [3] C. H. Bennett and D. P. DiVincenzo, Quantum information and computation, *Nature (London)* **404**, 247 (2000).
 [4] C. H. Bennett, G. Brassard, C. Crépeau, R. Jozsa, A. Peres, and W. K. Wootters, Teleporting an Unknown Quantum State via Dual Classical and Einstein-Podolsky-Rosen Channels, *Phys. Rev. Lett.* **70**, 1895 (1993).

[5] V. Scarani, H. Bechmann-Pasquinucci, N. J. Cerf, M. Dušek, N. Lütkenhaus, and M. Peev, The security of practical quantum key distribution, *Rev. Mod. Phys.* **81**, 1301 (2009).
 [6] R. P. Feynman, Simulating physics with computers, *Int. J. Theor. Phys.* **21**, 467 (1982).
 [7] D. Deutsch, Quantum theory, the Church-Turing principle and the universal quantum computer, *Proc. R. Soc. London A* **400**, 97 (1985).
 [8] X.-Y. Luo, Y.-Q. Zou, L.-N. Wu, Q. Liu, M.-F. Han, M. K. Tey, and L. You, Deterministic entanglement generation from

- driving through quantum phase transitions, *Science* **355**, 620 (2017).
- [9] F. Arute, K. Arya, R. Babbush, D. Bacon, J. C. Bardin, R. Barends, R. Biswas, S. Boixo, F. G. Brandao, D. A. Buell *et al.*, Quantum supremacy using a programmable superconducting processor, *Nature (London)* **574**, 505 (2019).
- [10] C.-M. Li, K. Chen, A. Reingruber, Y.-N. Chen, and J.-W. Pan, Verifying Genuine High-Order Entanglement, *Phys. Rev. Lett.* **105**, 210504 (2010).
- [11] X.-C. Yao, T.-X. Wang, P. Xu, H. Lu, G.-S. Pan, X.-H. Bao, C.-Z. Peng, C.-Y. Lu, Y.-A. Chen, and J.-W. Pan, Observation of eight-photon entanglement, *Nat. Photon.* **6**, 225 (2012).
- [12] M. Gong, S. Wang, C. Zha, M.-C. Chen, H.-L. Huang, Y. Wu, Q. Zhu, Y. Zhao, S. Li, S. Guo, H. Qian, Y. Ye, F. Chen, C. Ying, J. Yu, D. Fan, D. Wu, H. Su, H. Deng, H. Rong *et al.*, Quantum walks on a programmable two-dimensional 62-qubit superconducting processor, *Science* **372**, 948 (2021).
- [13] S. Yokoyama, R. Ukai, S. C. Armstrong, C. Sornphiphatphong, T. Kaji, S. Suzuki, J.-I. Yoshikawa, H. Yonezawa, N. C. Menicucci, and A. Furusawa, Ultra-large-scale continuous-variable cluster states multiplexed in the time domain, *Nat. Photon.* **7**, 982 (2013).
- [14] B. Lücke, J. Peise, G. Vitagliano, J. Arlt, L. Santos, G. Tóth, and C. Klempt, Detecting Multiparticle Entanglement of Dicke States, *Phys. Rev. Lett.* **112**, 155304 (2014).
- [15] J. Preskill, Quantum computing in the NISQ era and beyond, *Quantum* **2**, 79 (2018).
- [16] A. Peres, Separability Criterion for Density Matrices, *Phys. Rev. Lett.* **77**, 1413 (1996).
- [17] P. Horodecki, Separability criterion and inseparable mixed states with positive partial transposition, *Phys. Lett. A* **232**, 333 (1997).
- [18] K. Chen and L.-A. Wu, A matrix realignment method for recognizing entanglement, *Quantum Inform. Comput.* **3**, 193 (2003).
- [19] O. Rudolph, Further results on the cross norm criterion for separability, *Quantum Inf. Process.* **4**, 219 (2005).
- [20] K. Chen, S. Albeverio, and S.-M. Fei, Concurrence of Arbitrary Dimensional Bipartite Quantum States, *Phys. Rev. Lett.* **95**, 040504 (2005).
- [21] K. Chen, S. Albeverio, and S.-M. Fei, Entanglement of Formation of Bipartite Quantum States, *Phys. Rev. Lett.* **95**, 210501 (2005).
- [22] M. B. Plenio and S. S. Virmani, An introduction to entanglement theory, *Quantum Inform. Comput.* **7**, 1 (2007).
- [23] O. Gühne and G. Tóth, Entanglement detection, *Phys. Rep.* **474**, 1 (2009).
- [24] N. Friis, G. Vitagliano, M. Malik, and M. Huber, Entanglement certification from theory to experiment, *Nat. Rev. Phys.* **1**, 72 (2019).
- [25] N. Brunner, J. Sharam, and T. Vértesi, Testing the Structure of Multipartite Entanglement with Bell Inequalities, *Phys. Rev. Lett.* **108**, 110501 (2012).
- [26] Y. Zhou, Q. Zhao, X. Yuan, and X. Ma, Detecting multipartite entanglement structure with minimal resources, *npj Quantum Inf.* **5**, 83 (2019).
- [27] M. Horodecki, P. Horodecki, and R. Horodecki, Separability of mixed states: necessary and sufficient conditions, *Phys. Lett. A* **223**, 1 (1996).
- [28] B. M. Terhal, Bell inequalities and the separability criterion, *Phys. Lett. A* **271**, 319 (2000).
- [29] M. Lewenstein, B. Kraus, J. I. Cirac, and P. Horodecki, Optimization of entanglement witnesses, *Phys. Rev. A* **62**, 052310 (2000).
- [30] P. Hyllus, O. Gühne, D. Bruß, and M. Lewenstein, Relations between entanglement witnesses and Bell inequalities, *Phys. Rev. A* **72**, 012321 (2005).
- [31] M. Lewenstein, B. Kraus, P. Horodecki, and J. I. Cirac, Characterization of separable states and entanglement witnesses, *Phys. Rev. A* **63**, 044304 (2001).
- [32] O. Gühne, M. Reimpell, and R. F. Werner, Estimating Entanglement Measures in Experiments, *Phys. Rev. Lett.* **98**, 110502 (2007).
- [33] N. Friis, O. Marty, C. Maier, C. Hempel, M. Holzäpfel, P. Jurcevic, M. B. Plenio, M. Huber, C. Roos, R. Blatt, and B. Lanyon, Observation of Entangled States of a Fully Controlled 20-Qubit System, *Phys. Rev. X* **8**, 021012 (2018).
- [34] T. Monz, P. Schindler, J. T. Barreiro, M. Chwalla, D. Nigg, W. A. Coish, M. Harlander, W. Hänsel, M. Hennrich, and R. Blatt, 14-Qubit Entanglement: Creation and Coherence, *Phys. Rev. Lett.* **106**, 130506 (2011).
- [35] N. Kiesel, C. Schmid, U. Weber, G. Tóth, O. Gühne, R. Ursin, and H. Weinfurter, Experimental Analysis of a Four-Qubit Photon Cluster State, *Phys. Rev. Lett.* **95**, 210502 (2005).
- [36] W.-B. Gao, C.-Y. Lu, X.-C. Yao, P. Xu, O. Gühne, A. Goebel, Y.-A. Chen, C.-Z. Peng, Z.-B. Chen, and J.-W. Pan, Experimental demonstration of a hyper-entangled ten-qubit Schrödinger cat state, *Nat. Phys.* **6**, 331 (2010).
- [37] H. Lu, Q. Zhao, Z.-D. Li, X.-F. Yin, X. Yuan, J.-C. Hung, L.-K. Chen, L. Li, N.-L. Liu, C.-Z. Peng, Y.-C. Liang, X. Ma, Y.-A. Chen, and J.-W. Pan, Entanglement Structure: Entanglement Partitioning in Multipartite Systems and Its Experimental Detection Using Optimizable Witnesses, *Phys. Rev. X* **8**, 021072 (2018).
- [38] Z.-D. Li, Q. Zhao, R. Zhang, L.-Z. Liu, X.-F. Yin, X. Zhang, Y.-Y. Fei, K. Chen, N.-L. Liu, F. Xu, Y.-A. Chen, L. Li, and J.-W. Pan, Measurement-Device-Independent Entanglement Witness of Tripartite Entangled States and Its Applications, *Phys. Rev. Lett.* **124**, 160503 (2020).
- [39] M. Gong, M.-C. Chen, Y. Zheng, S. Wang, C. Zha, H. Deng, Z. Yan, H. Rong, Y. Wu, S. Li, F. Chen, Y. Zhao, F. Liang, J. Lin, Y. Xu, C. Guo, L. Sun, A. D. Castellano, H. Wang, C. Peng *et al.*, Genuine 12-Qubit Entanglement on a Superconducting Quantum Processor, *Phys. Rev. Lett.* **122**, 110501 (2019).
- [40] D. M. Greenberger, M. A. Horne, and A. Zeilinger, Going beyond Bell's theorem, in *Bell's Theorem, Quantum Theory and Conceptions of the Universe*, edited by M. Kafatos (Springer Netherlands, Dordrecht, The Netherlands, 1989), pp. 69–72.
- [41] W. Dür, G. Vidal, and J. I. Cirac, Three qubits can be entangled in two inequivalent ways, *Phys. Rev. A* **62**, 062314 (2000).
- [42] M. Hein, J. Eisert, and H. J. Briegel, Multipartite entanglement in graph states, *Phys. Rev. A* **69**, 062311 (2004).
- [43] M. Hein, W. Dür, J. Eisert, R. Raussendorf, M. V. den Nest, and H. J. Briegel, Entanglement in graph states and its applications, [arXiv:quant-ph/0602096](https://arxiv.org/abs/quant-ph/0602096).
- [44] M. Bourennane, M. Eibl, C. Kurtsiefer, S. Gaertner, H. Weinfurter, O. Gühne, P. Hyllus, D. Bruß, M. Lewenstein, and A. Sanpera, Experimental Detection of Multipartite Entanglement using Witness Operators, *Phys. Rev. Lett.* **92**, 087902 (2004).

- [45] B. Jungnitsch, T. Moroder, and O. Gühne, Taming Multiparticle Entanglement, *Phys. Rev. Lett.* **106**, 190502 (2011).
- [46] M. Huber and R. Sengupta, Witnessing Genuine Multipartite Entanglement with Positive Maps, *Phys. Rev. Lett.* **113**, 100501 (2014).
- [47] J. Sperling and W. Vogel, Multipartite Entanglement Witnesses, *Phys. Rev. Lett.* **111**, 110503 (2013).
- [48] M. Weilenmann, B. Dive, D. Trillo, E. A. Aguilar, and M. Navascués, Entanglement Detection beyond Measuring Fidelities, *Phys. Rev. Lett.* **124**, 200502 (2020).
- [49] C. Lancien, O. Gühne, R. Sengupta, and M. Huber, Relaxations of separability in multipartite systems: Semidefinite programs, witnesses and volumes, *J. Phys. A: Math. Theor.* **48**, 505302 (2015).
- [50] F. Clivaz, M. Huber, L. Lami, and G. Murta, Genuine-multipartite entanglement criteria based on positive maps, *J. Math. Phys.* **58**, 082201 (2017).
- [51] M. Bergmann and O. Gühne, Entanglement criteria for Dicke states, *J. Phys. A: Math. Theor.* **46**, 385304 (2013).
- [52] H. J. Briegel, D. E. Browne, W. Dür, R. Raussendorf, and M. Van den Nest, Measurement-based quantum computation, *Nat. Phys.* **5**, 19 (2009).
- [53] D. Schlingemann and R. F. Werner, Quantum error-correcting codes associated with graphs, *Phys. Rev. A* **65**, 012308 (2001).
- [54] B. Jungnitsch, T. Moroder, and O. Gühne, Entanglement witnesses for graph states: General theory and examples, *Phys. Rev. A* **84**, 032310 (2011).
- [55] O. Gühne, Y. Mao, and X.-D. Yu, Geometry of Faithful Entanglement, *Phys. Rev. Lett.* **126**, 140503 (2021).
- [56] Y. Zhan and H.-K. Lo, Detecting entanglement in unfaithful states, [arXiv:2010.06054](https://arxiv.org/abs/2010.06054).
- [57] G. Riccardi, D. E. Jones, X.-D. Yu, O. Gühne, and B. T. Kirby, Exploring the relationship between the faithfulness and entanglement of two qubits, *Phys. Rev. A* **103**, 042417 (2021).
- [58] X.-M. Hu, W.-B. Xing, Y. Guo, M. Weilenmann, E. A. Aguilar, X. Gao, B.-H. Liu, Y.-F. Huang, C.-F. Li, G.-C. Guo, Z. Wang, and M. Navascués, Optimized Detection of High-Dimensional Entanglement, *Phys. Rev. Lett.* **127**, 220501 (2021).
- [59] Y. Dai, Y. Dong, Z. Xu, W. You, C. Zhang, and O. Gühne, Experimentally Accessible Lower Bounds for Genuine Multipartite Entanglement and Coherence Measures, *Phys. Rev. Appl.* **13**, 054022 (2020).
- [60] M. Navascués, E. Wolfe, D. Rosset, and A. Pozas-Kerstjens, Genuine Network Multipartite Entanglement, *Phys. Rev. Lett.* **125**, 240505 (2020).
- [61] T. Kraft, S. Designolle, C. Ritz, N. Brunner, O. Gühne, and M. Huber, Quantum entanglement in the triangle network, *Phys. Rev. A* **103**, L060401 (2021).
- [62] P. Contreras-Tejada, C. Palazuelos, and J. I. de Vicente, Asymptotic Survival of Genuine Multipartite Entanglement in Noisy Quantum Networks Depends on the Topology, *Phys. Rev. Lett.* **128**, 220501 (2022).
- [63] R. Augusiak, J. Tura, and M. Lewenstein, A note on the optimality of decomposable entanglement witnesses and completely entangled subspaces, *J. Phys. A: Math. Theor.* **44**, 212001 (2011).
- [64] G. Vidal and R. Tarrach, Robustness of entanglement, *Phys. Rev. A* **59**, 141 (1999).